energies

MDPI

Article

Study on the Combustion Behavior of Inhomogeneous Partially Premixed Mixtures in Confined Space

Yanfei Li [1], Xin Zhang [1,*], Lichao Chen [2] and Ying Liu [1]

[1] Beijing Key Laboratory of Powertrain for New Energy Vehicle, School of Mechanical Electronic and Control Engineering, Beijing Jiaotong University, Beijing 100044, China; 20116042@bjtu.edu.cn (Y.L.); 23121359@bjtu.edu.cn (Y.L.)

[2] School of Mechanical Engineering, Beijing Institute of Technology, Beijing 100081, China; lcchen2011@126.com

* Correspondence: zhangxin@bjtu.edu.cn; Tel.: +86-10-51688404

Abstract: Reasonably configuring the concentration distribution of the mixture to achieve partially premixed combustion has been proven to be an effective method for improving energy utilization efficiency. However, due to the significant influence of concentration non-uniformity and flow field disturbances, the combustion behavior and mechanisms of partially premixed combustion have not been fully understood or systematically analyzed. In this study, the partially premixed combustion characteristics of methane–hydrogen–air mixtures in a confined space were investigated, focusing on the combustion behavior and key parameter variation patterns under different equivalence ratios (0.5, 0.7, 0.9) and hydrogen contents (10%, 20%, 30%, 40%). The global equivalence ratio and degree of partial premixing of the mixture were controlled by adjusting the fuel injection pulse width and ignition timing, thereby regulating the concentration field and flow field distribution within the combustion chamber. The constant-pressure method was used to calculate the burning velocity. Results show that as the mixture formation time decreases, the degree of partial premixing increases, accelerating the heat release process, increasing burning velocity, and shortening the combustion duration. It exhibits rapid combustion characteristics, particularly during the initial combustion phase, where flame propagation speed and heat release rate increase significantly. The burning velocity demonstrates a distinct single-peak profile, with the peak burning velocity increasing and its occurrence advancing as the degree of partial premixing increases. Additionally, hydrogen's preferential diffusion effect is enhanced with increasing mixture partial premixing, making the combustion process more efficient and concentrated. This effect is particularly pronounced under low-equivalence-ratio (lean burn) conditions, where the combustion reaction rate improves more significantly, leading to greater combustion stability. The peak of the partially premixed burning velocity occurs almost simultaneously with the peak of the second-order derivative of the combustion pressure. This phenomenon highlights the strong correlation between the combustion reaction rate and the dynamic variations in pressure.

Keywords: constant-volume combustion bomb; partially premixed combustion; methane and hydrogen; burning velocity; rapid combustion

check for updates

Academic Editor: Roberto Finesso

Received: 31 December 2024
Revised: 8 February 2025
Accepted: 11 February 2025
Published: 13 February 2025

Citation: Li, Y.; Zhang, X.; Chen, L.; Liu, Y. Study on the Combustion Behavior of Inhomogeneous Partially Premixed Mixtures in Confined Space. *Energies* **2025**, *18*, 899. https://doi.org/10.3390/en18040899

Copyright: © 2025 by the authors. Licensee MDPI, Basel, Switzerland. This article is an open access article distributed under the terms and conditions of the Creative Commons Attribution (CC BY) license (https://creativecommons.org/licenses/by/4.0/).

1. Introduction

New energy conversion technologies such as lithium battery technology [1] and fuel cell technology [2] have made great progress in recent years. However, constrained by factors such as energy density, material costs, production scale, and charging infrastructure, internal combustion engines (ICEs) will continue to play a dominant role in sectors such as

transportation, construction machinery, and defense industries for the foreseeable future. Particularly in commercial vehicles and hybrid electric vehicles, ICEs, with their high-power density, rapid response, and strong reliability, remain a crucial bridge for achieving energy transition in the future [3]. However, with the increasing severity of energy shortages and environmental pollution, the ICEs are facing significant challenges, necessitating the exploration of innovative combustion technologies to enhance energy efficiency.

In practical combustion systems, due to temporal and spatial constraints, fuel and oxidizers often cannot achieve complete mixing, complicating the combustion process and resulting in the combustible mixture primarily existing in a partially premixed combustion state. A reasonable configuration of the concentration distribution of the mixture in the combustion chamber can improve combustion performance and increase energy utilization [4]. For example, the direct injection technology in internal combustion engine cylinders allows for highly controllable localized stratified fuel distribution by precisely regulating the timing and mode of fuel injection, thereby enabling partially premixed combustion [5]. The core advantage of this technology lies in its ability to flexibly adjust the concentration and flow fields of the mixture within the combustion chamber, effectively controlling the burning velocity. This is particularly beneficial under lean-burn conditions, as it significantly enhances combustion stability [6].

Although the advantages of partially premixed combustion have been widely recognized, the combustible mixtures in the combustion chambers of different engine types have strong spatial nonuniformity and time-varying instability, and it is difficult to have a strong generalization of the study results. In order to study partially premixed combustion behavior, many scholars have developed some specific combustion apparatuses, such as a Darmstadt stratified combustor [7], Cambridge/Sandia swirl [8] and non-swirl [9] combustion devices, a modified Sydney inhomogeneous pilot burner [10], and so on. Based on these specific combustion devices, researchers have conducted a series of experimental studies, obtaining extensive data on flame characteristics and combustion processes [11].

The above combustor creates the partially premixed flame by varying the equivalence ratios of the mixtures at different outlets, which allows for an in-depth study of stratified flame characteristics in unconfined spaces. It is quite different from the approximate spherical flame propagation process in the real ICE combustion chamber confined space. The combustion behavior and combustion mechanism of partially premixed combustion processes in confined spaces similar to the combustion chamber environment of ICEs still require further investigation.

The study of combustion characteristics in confined spaces is of great significance for understanding the combustion behavior in practical ICEs. The constant-volume combustion bomb is a simplified device for the combustion chambers of ICEs to avoid the influence of the combustion chamber structure and the intake and exhaust processes on the combustion efficiency. By decoupling multiple variables in complex combustion processes, the constant-volume combustion chamber (CVCC) provides an ideal platform for in-depth investigations of burning velocity, pressure variations, and heat release characteristics [12]. Pasquier et al. [13] investigated the propagation characteristics of the propane–air flame through inhomogeneous mixtures in a confined space. The results showed that concentration-stratified mixtures (chemical equivalence ratio to lean) accelerated the global flame propagation compared to the flame propagation process in homogeneous mixtures. Balusamy et al. [14] measured the flame burning velocity at three levels of stratification (mixture equivalence ratios are 1.24, 0.95, and 0.8 in the ignition region) under the constant-volume conditions using the simultaneous PIV-PLIF technique [15]. The results show that the flame will be back-supported for a longer period of time when ignited in the richer region for inhomogeneous lean mixtures. The results indicate that

the concentration gradient of the mixture has a significant impact on combustion stability. Wang et al. [16] found that the combination of partially premixed direct injection and a hydrogen addition can achieve stable ignition and fast combustion in lean mixtures. The burning velocity decreases with the increase in the premix ratio and increases with the increase in hydrogen content. Askari et al. investigated the turbulent partially premixed combustion characteristics of methane–air [17] and methane–hydrogen–air [18] under constant-volume conditions. The results show that the turbulent field intensity at the ignition moment is greater by reducing the ignition delay period. This contributes to a shorter combustion duration and higher combustion pressure during turbulent partially premixed combustion. Lee et al. [19] carried out hydrogen partially premixed combustion experiments in a confined space. The local equivalence ratio and the morphology of the hydrogen jet are the key parameters of the hydrogen partially premixed combustion process. The combustion can be optimized by adjusting the injection and ignition moments. Ge et al. [20] investigated the ignition characteristics of hydrogen–ethanol partially premixed ultra-lean combustion for different ignition times (0~50 ms after the start of injection), injection pressures (5, 15, and 25 MPa), and hydrogen premixing equivalence ratios (0.05, 0.1, and 0.2). Fuel stratification and hydrogen addition increased the stabilized ignition limit to an ultra-lean state.

The above studies have paid more attention to the global burning velocity and combustion duration. The evolution of burning velocity and its influencing factors during partially premixed combustion has rarely been analyzed and studied, which will be investigated in depth in this paper.

Burning velocity is an important parameter for evaluating combustion efficiency. Due to the effects of a non-homogeneous concentration field and disturbance turbulence field, the non-homogeneous partially premixed combustion velocity in the confined space is exceptionally complex, and its definition and calculation method are crucial.

The flame morphology in the confined space is an outward propagating spherical flame. In the early stages, the flame curvature/stretching effects are significant, and the rise in combustion pressure can be neglected. Afterward, the combustion pressure rise rate increases significantly, and the flame curvature/stretching effects become negligible. Based on the design of the combustion chamber and the process of combustion pressure rise, there are two main methods to measure burning velocity using spherical flames; one is the constant-pressure method [21,22] and the other is the constant-volume method [23].

In the constant-pressure method, which is mainly applicable to the initial stage of combustion, high-speed cameras are used to capture images of the combustion flame, and data on the flame front evolution are extracted from these images to obtain the unstretched burning velocity [24]. As combustion further develops, the suppression of flame development by combustion pressure becomes significant, making this method no longer applicable. Additionally, the density ratio at the flame front is required by using the constant-pressure method. In actual internal combustion engine setups, the concentration distribution of the mixture within the combustion chamber is uneven and changes in real time, making it difficult to obtain a clear density ratio [25]. Therefore, this method is only applicable to homogeneous premixed combustion processes. At the same time, researchers are more interested in obtaining the global burning velocity characteristics of partially premixed mixtures to evaluate the combustion performance of actual combustion devices.

In comparison, the constant-volume method derives the burning velocity based on the dynamic changes in combustion pressure, making it effectively applicable throughout the entire combustion process. Although the constant-volume method may introduce some errors during the initial and final stages of combustion due to the relatively small changes in combustion pressure, it still provides an accurate estimate of the burning veloc-

ity for partially premixed combustion. This method was first proposed by Lewis and von Elba [26] in 1934. Saee [27], A. Omari [28], and N. Hinton [29] also compared the accuracy of laminar burning velocities using the constant-volume method and the constant-pressure method to confirm the reliability of the constant-volume method. The literature [30] provides a review of the constant-volume method. Reyes et al. [31] investigated the burning velocities of methane–air and hydrogen–air mixtures at different initial pressures, temperatures, and fuel/air equivalence ratios in a spherical constant-volume combustion bomb. Sun et al. [32] investigated the turbulent burning characteristics of methane–hydrogen [33] and syngas [34] mixtures in a spherical constant-volume combustion vessel, further extending the applicability of this method. This method has been widely used in constant-volume combustion equipment [34–37] and engines [38,39].

Many scholars have paid more attention to the study of laminar or turbulent burning velocity in the premixed combustion process in confined spaces, but the partially premixed combustion behavior prevalent within actual combustion equipment has been less studied and requires further research. The authors investigated the flame propagation speed and stability of the initial stage (constant-pressure combustion) of the partially premixed combustion process by using a constant-volume combustion bomb experimental platform. The combustion behavior of partially premixed mixtures throughout the combustion process (constant-volume combustion) will be further analyzed in this study.

In this study, the partially premixed combustion behavior of the inhomogeneous lean methane–hydrogen–air mixtures in a confined space was experimentally investigated. Pure fuel was injected into the combustion bomb using a high-pressure injection valve to form a lean partially premixed mixture. The global equivalence ratio was controlled by adjusting the injection pulse width, while the degree of partial premixing was manipulated by varying the mixture formation time (ignition delay). Burning velocity was calculated using the constant-pressure method based on pressure signal measurements. The effects of the global equivalence ratio (0.5, 0.7, 0.9), hydrogen content (10%, 20%, 30%, 40%), and partial premixing levels (mixture formation times of 10 ms, 50 ms, 100 ms, 200 ms, and 3 min) on the partially premixed combustion process were analyzed. Furthermore, the rapid combustion behavior and heat release dynamics of partially premixed methane–hydrogen–air mixtures were investigated. The evolution of burning velocity and the influence of mixture composition (equivalence ratio and hydrogen content) and the partial premixing degree on burning velocity were investigated. The correlation between burning velocity and combustion pressure was analyzed. These findings offer critical experimental data and theoretical insights for enhancing the stability and efficiency of partially premixed combustion in combustion chambers of ICEs.

2. Methodology

2.1. Experimental Apparatus

The experiments in this study were conducted on a nearly spherical constant-volume combustion bomb experimental platform. This experimental platform mainly consisted of a constant-volume combustion chamber (CVCC), gas distribution system, ignition system, timing control system, and data acquisition system, as shown in Figure 1.

The CVCC had an approximately spherical inner cavity with a radius of 100 mm and a volume of about 6.38 L. On both the front and back sides of the CVCC were cylindrical cavities with a radius of 50 mm, designed to hold high-strength quartz glass, which served as the optical path for the schlieren system to observe flame morphology. The gas distribution system of the experimental platform consisted of high-pressure gas cylinders, pressure-reducing valves, switch valves, pressure gauges, a pressure-stabilizing chamber, and a modified high-pressure fuel injector (06F906036A). That fuel injector was installed

on the top of the chamber to inject fuel into the CVCC. Given that natural gas has a lower density than conventional gasoline and diesel fuels, the injection hole diameter was modified to 1 mm to increase the injection volume.

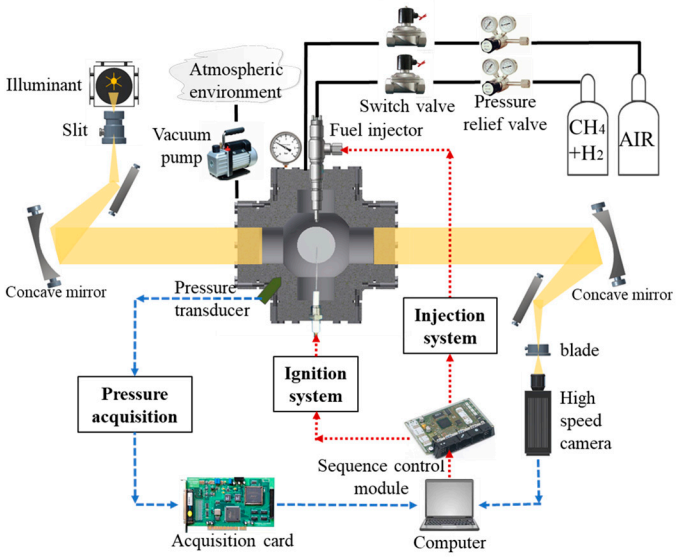


Figure 1. Schematic diagram of experimental platform of constant-volume combustion bomb.

The ignition electrode was located at the center of the combustion chamber. The pulse width of the ignition pulse signal could be controlled to adjust the ignition energy. In this study, the pulse width of the ignition pulse signal was set to 12 ms, resulting in an ignition energy of 284 mJ. The DG535 digital delay generator was used in the timing control system to precisely control timing signals such as injection pulse width and ignition timing, thereby igniting mixtures with different partial premixing degrees while synchronously collecting flame images and combustion pressure signals. The DG535 digital delay generator allows for settings of delay times and pulse widths with a precision of up to 5 ps.

The schlieren system [40], combined with a high-speed camera (IDT Motion Pro-Y4) and an AF-S NIKKOR 50 mm F1.4G full-frame fixed-focus lens, was used to capture real-time flame images. The schlieren system's optical path was arranged in a Z-shape, with the CVCC located in the middle of the optical path. A pressure sensor (Kistler 6061B) was mounted on the wall of the CVCC. The charge signal from the pressure sensor was amplified by a charge amplifier and transmitted to a computer via a PCI1710U data acquisition card, enabling the real-time collection of combustion pressure signals during the combustion process.

The initial temperature of the experimental process was set to 298 K, and the initial pressure was 0.1 MPa. Air was first charged into the combustion chamber, followed by the injection of methane–hydrogen mixed fuel with varying hydrogen content through the fuel injector located directly above the center of the CVCC, forming a combustible mixture. At a specific moment, the combustible mixture was ignited, and the data acquisition system was triggered simultaneously. The schematic diagram of the timing signal control is shown in Figure 2. The fuel injection pressure was set to 6 MPa. The pulse width of the fuel injection could be controlled to adjust the global equivalence ratio of the mixture inside the chamber. The mixture formation time (*MFT*) is defined as the time between the end of fuel injection and the ignition moment. In this study, the mixture formation times were set to 10 ms, 50 ms, 100 ms, 200 ms, and 3 min. When the *MFT* was 3 min, the fuel had sufficient time to diffuse, and the flow field inside the combustion chamber became nearly stable, resulting in a laminar premixed combustion process. When the *MFT* was relatively short, the concentration distribution within the combustion chamber became inhomogeneous,

accompanied by flow disturbances. Under such conditions, the combustion process was characterized as partially premixed combustion [41]. As the *MFT* decreased, the degree of partial premixing of the mixture in the CVCC increased. The experimental related parameter settings are shown in Table 1.

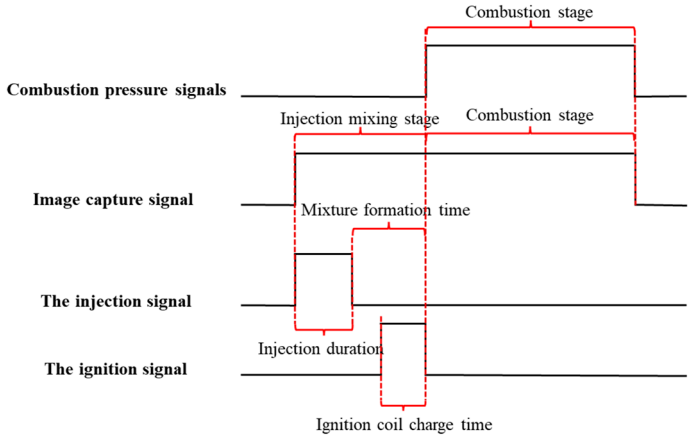


Figure 2. Schematic diagram of timing signal control.

Table 1. Experiment-related parameter settings.

Parameter	Value
Methane Concentration	99.999%
Methane Temperature	298 K
Hydrogen Concentration	99.99%
Hydrogen Temperature	298 K
Ambient Pressure	0.1 MPa
Ambient Temperature	298 K
Fuel Injection Pressure	6 MPa
Global Equivalence Ratio of the Mixture	0.5, 0.7, 0.9
Hydrogen Content of the Mixture	10%, 20%, 30%, 40%
Mixture Formation Time	10 ms, 50 ms, 100 ms, 200 ms, 3 min
Flame Image Capture Pixel Resolution	512 × 512
Flame Image Capture Frequency	5000 HZ
Pressure Data Acquisition Frequency	30000 HZ

In the gas charging process, the vacuum pump is first used to evacuate the air from the combustion chamber to achieve a near-vacuum state (with an absolute pressure of around 0.005 MPa). Then, the calculated amounts of fuel and oxidizer are charged. During the experiment, the volume fractions of each component gas are calculated using Dalton's law of partial pressures and the ideal gas law [42]. The hydrogen content X_{H2} in the fuel is calculated using the following formula:

$$X_{H2} = \frac{V_{H2}}{V_{H2} + V_{CH4}} = \frac{P_{H2}}{P_{H2} + P_{CH4}} \tag{1}$$

where V_{H2} is the volume fraction of hydrogen and V_{CH4} is the volume fraction of methane. P_{H2} and P_{CH4} are the partial pressures of hydrogen and methane, respectively.

According to Dalton's law of partial pressures, the partial pressures of methane, hydrogen, oxygen, and nitrogen in the combustible mixture are proportional to its molar amounts. The partial pressures of each component can be represented as

$$P_{CH4} : P_{H2} : P_{O2} : P_{N2} = \varphi(1 - X_{H2}) : \varphi X_{H2} : (2 - \frac{3}{2}X_{H2}) : 3.762(2 - \frac{3}{2}X_{H2}) \tag{2}$$

The partial pressure of the air (oxygen and nitrogen) in the CVCC is equal to the initial pressure of the mixture, given by

$$P_{O2} + P_{N2} = P_i \tag{3}$$

where P_i is the initial pressure of the chamber, which is 0.1 MPa in this study. By solving the above equations, the partial pressures of each component in the mixture can be calculated.

The fuel injection is located directly above the center of the CVCC, with the nozzle direction pointed vertically downward. This study uses a single-hole, non-tilted, high-pressure fuel injector. The inner cavity of the CVCC is approximately spherical, which ensures that the concentrations of the mixture and the flame propagation are nearly symmetrical around the circumference. This design minimizes the influence of the internal structure of the CVCC on the flame propagation process.

The jet characteristics of methane–hydrogen mixtures with different hydrogen contents are as shown in Figure 3. For the same fuel composition, the fuel injection quantity exhibits a linear relationship with the injection pulse width. As the hydrogen content in the mixed fuel increases, the slope gradually decreases. This is because the molar mass of hydrogen (2 g/mol) is much smaller than that of methane (16 g/mol). Based on the injection characteristics of different fuels, the injection pulse width required to create combustible mixtures with different equivalence ratios can be calculated. With an increase in hydrogen content in the mixed fuel, achieving the same equivalence ratio for the combustible mixture requires a longer injection pulse width. This is mainly because the oxygen required for the complete combustion of hydrogen is only one-quarter of that required for methane combustion.

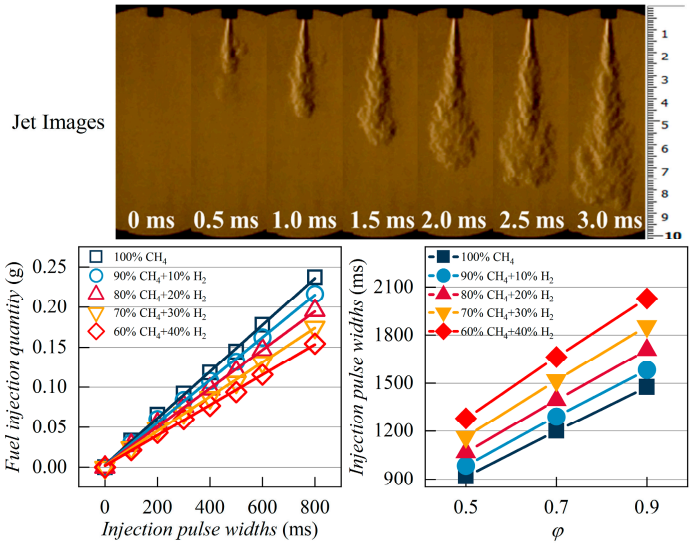


Figure 3. The jet characteristics of different fuels.

Before conducting the experiments, it is essential to validate the reliability of the experimental platform. Figure 4 shows the flame image experimental results obtained using this platform. The operating conditions are an *MFT* of 50 ms and an equivalence ratio of 0.85 for pure methane in a partially premixed combustion process. The flow disturbances and the inhomogeneous concentration distribution caused by the fuel jet led to the formation of wrinkles and cellular structures in the flame front, accelerating the flame propagation speed. This structure not only reflects the enhancement effect of turbulence on flame propagation but also highlights the significant impact of local concentration gradients on the chemical reaction rate. This demonstrates the strong coupling between the flow field,

concentration field, and combustion reactions in the partially premixed combustion process. Although there are slight differences in the development of the local flame structure during different testing processes, the macroscopic cellular structures, wrinkle patterns, and flame propagation speed of the flame front are almost identical. Some errors and uncertainties inevitably arise during the experiment. The initial temperature and pressure errors are ± 3 K and ± 0.1 kPa, respectively. The uncertainty in the combustion pressure measured by the Kistler 6061B pressure sensor is $\pm 0.8\%$. The precision of the injection and flame images is 0.25 mm/pixel. To improve accuracy, the experiments were repeated three times in this study.

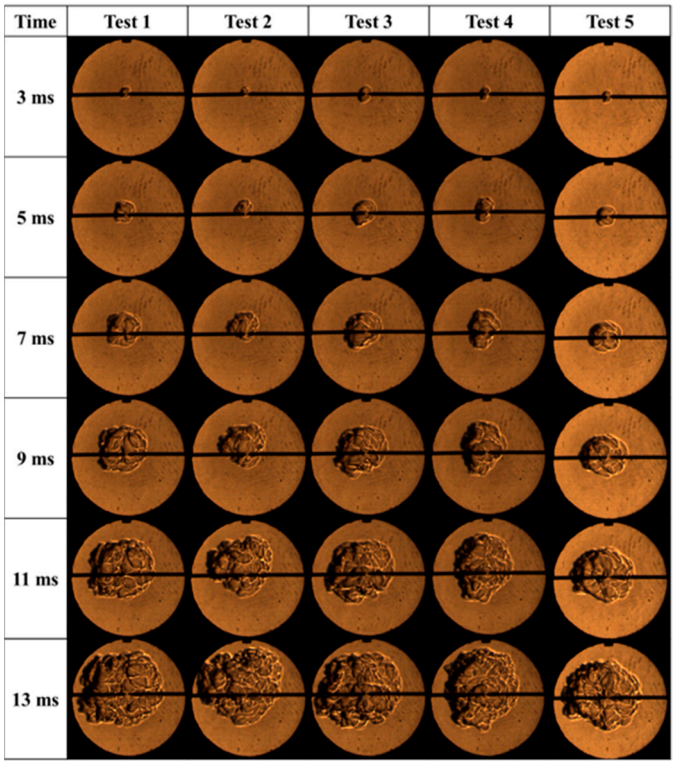


Figure 4. Repeatability experimental results of flame image.

2.2. Calculation of Partially Premixed Burning Velocity

In this paper, the constant-pressure method [43] is used to calculate the burning velocities of the partially premixed combustion process of the methane–hydrogen–air mixtures under different operating conditions. This method estimates the burning velocity based on the dynamic variation in the pressure signal during combustion and can accurately reflect the heat release and combustion kinetics characteristics. However, to ensure the validity of the calculations, several assumptions are typically required. Firstly, it is assumed that the pressure remains spatially uniform throughout the combustion process, meaning that the pressure distribution inside the combustion chamber is considered homogeneous and local pressure gradients are not taken into account. Although local disturbances may exist in practical combustion processes, this assumption is generally a reasonable approximation in a closed system. Secondly, it is assumed that the total mass of the mixture within the combustion chamber remains unchanged, meaning that the total mass of the unburned gasses and combustion products does not vary throughout the combustion process. This assumption neglects product diffusion losses, which is typically valid in a confined environment. Additionally, it is assumed that the combustion system is not subject to external heat input, that heat loss at the combustion chamber walls is negligible, and that buoyancy effects on flame propagation can be ignored. This assumption is particularly reasonable

in small-scale combustion chambers or under high-pressure conditions. Regarding flame propagation characteristics, the flame front is assumed to be approximately spherical and infinitely thin, allowing the calculation of burning velocity to be based on the variation in the spherical flame front radius. However, in actual partially premixed combustion, the flame may develop wrinkles or cellular structures due to turbulence and concentration gradients, potentially leading to localized deviations in burning velocity. Furthermore, it is assumed that the unburned gasses undergo isentropic compression during combustion, meaning that their state changes follow an isentropic process, neglecting irreversible losses and heat conduction effects, thereby simplifying the combustion pressure–volume relationship calculations. Lastly, it is assumed that the composition and temperature of the mixture in the burned and unburned regions have certain mean values but continuously evolve with flame propagation. This assumption allows for the use of average state variables in burning velocity calculations, providing a reasonable estimation.

The constant-pressure method employed in this study calculates the partially premixed burning velocity based on the combustion pressure signal, which effectively reflects the combustion process of the mixture. Although the aforementioned assumptions may introduce some degree of error, such as deviations from an ideal spherical flame front or the influence of wall heat loss, these errors can generally be neglected or compensated for through correction methods when experimental conditions are properly controlled. This ensures the accuracy and reliability of the calculated results.

The burning velocity S_T can be calculated by the following formula:

$$\rho_u A_b S_T = -\frac{dm_u}{dt} \tag{4}$$

where A_b is the area of the flame front; ρ_u and m_u are the density and mass of the unburned mixture.

According to the mass conservation principle, the following calculation is determined:

$$-\frac{dm_u}{dt} = \frac{dm_b}{dt} = \rho_i V \frac{dx}{dt} \tag{5}$$

$$m_u = m_i - m_b = (1 - x) \cdot m_i \tag{6}$$

where V is the volume of the CVCC; m_i and ρ_i are the mass and density of the initial mixture in the combustion chamber; m_b and m_u are the mass of the burned and unburned mixture; and x is the combustion mass fraction.

$$\frac{dx}{dt} = \frac{dx}{dp} \times \frac{dp}{dt} \tag{7}$$

Combining the above Equations (4), (5), and (7), the following can be obtained:

$$\frac{dp}{dt} = \frac{A_b}{V} \frac{\rho_u}{\rho_i} \left(\frac{dx}{dp} \right)^{-1} S_T \tag{8}$$

The unburned mixture is isentropically compressed during the combustion process.

$$\frac{\rho_u}{\rho_i} = \left(\frac{p}{p_i} \right)^{1/\gamma_u} \tag{9}$$

$$\frac{T_u}{T_i} = \left(\frac{p}{p_i} \right)^{(\gamma_u - 1)/\gamma_u} \tag{10}$$

$$\gamma_u = c_{pu} / c_{vu} \tag{11}$$

where T_i and T_u are the temperatures of the initial and unburned mixture; c_{pu} and c_{vu} are the constant-pressure specific heat capacity and constant-volume specific heat capacity of the unburned mixture, respectively.

The flame is propagating in an approximately spherical shape, and the area A_b and volume V_b of the flame front are related to the radius R_b of the flame:

$$A_b = 4\pi R_b^2 \tag{12}$$

$$V_b = \frac{4}{3}\pi R_b^3 \tag{13}$$

Assuming that the initial mixture and the unburned mixture are ideal gasses, the equations of state are

$$p_i V = m_i R_u T_i \tag{14}$$

$$pV_u = m_u R_u T_u \tag{15}$$

where R_u is the gas constant of the unburned mixture.

Combining Equations (6), (14), and (15), the volume of the unburned mixture V_u can be calculated as

$$V_u = \frac{m_u R_u T_u}{p} = \frac{p_i}{p}\frac{T_u}{T_i}(1-x)V \tag{16}$$

Introducing the equalized radius R_v of the CVCC produces the following:

$$V = \frac{4 \cdot \pi \cdot R_v^3}{3} \tag{17}$$

The volume of the unburned mixture V_u can be obtained from volume conservation:

$$V_u = V - V_b = \frac{4\pi R_v^3}{3} - \frac{4\pi R_b^3}{3} = \frac{4\pi}{3}(R_v^3 - R_b^3) \tag{18}$$

The following can be obtained by combining Equations (16)–(18):

$$R_b = R_v\left[1 - (1-x)\frac{p_i}{p}\frac{T_u}{T_i}\right]^{1/3} \tag{19}$$

The area A_b-to-volume V_b ratio of the flame front is

$$\frac{A_b}{V_b} = \frac{3}{R_v}\left[1 - (1-x)\frac{p_i}{p}\frac{T_u}{T_i}\right]^{2/3} \tag{20}$$

Substituting Equations (9)–(11) and (20) into Equation (8) gives

$$\frac{dp}{dt} = \frac{3}{R_v}\left(\frac{dx}{dp}\right)^{-1}\left[1 - \left(\frac{p_i}{p}\right)^{1/\gamma_u}(1-x)\right]^{2/3}\left(\frac{p}{p_i}\right)^{1/\gamma_u} S_T \tag{21}$$

Substituting Equation (21) into Equation (7) to obtain the burning velocity S_T produces the following:

$$S_T = \frac{R_v}{3} \cdot \left[1 - (1-x) \cdot \left(\frac{p_i}{p}\right)^{1/\gamma_u}\right]^{-\frac{2}{3}} \cdot \left(\frac{p_i}{p}\right)^{1/\gamma_u} \cdot \frac{dx}{dt} \tag{22}$$

Lewis, B and Von Elbe, G [44] found an approximately linear relationship between the combustion mass fraction x and combustion pressure p:

$$x = \frac{p - p_i}{p_{\max} - p_i} \tag{23}$$

where $p_{\max}$ is the maximum pressure during the combustion process.

In order to improve the precision of burning velocity measurements, C.C.M. Luijtenet al. [45,46] proposed an analytical two-zone combustion model to obtain a modified equation for the combustion mass fraction versus pressure:

$$x = \frac{p - p_i f(p)}{p_{\max} - p_i f(p)} \tag{24}$$

$$f(p) = \left(\frac{\gamma_b - 1}{\gamma_u - 1}\right) + \left(\frac{\gamma_u - \gamma_b}{\gamma_u - 1}\right)\left(\frac{p}{p_i}\right)^{(\gamma_u - 1)/\gamma_u} \tag{25}$$

$$\gamma_b = c_{pb}/c_{vb} \tag{26}$$

where c_{pb} and c_{vb} are the constant-pressure specific heat capacity and constant-volume specific heat capacity of the burned mixture, respectively.

Combining the above Equations (22) and (24)–(26), the burning velocity S_T can be obtained.

3. Result and Discussion

3.1. Rapid Combustion Characteristics of Partially Premixed Combustion

Compared to a homogeneous premixed combustion process, the partially premixed combustion process of a non-homogeneous mixture results in an increased burning velocity, an accelerated heat release rate, and a shortened combustion duration, exhibiting distinct rapid combustion characteristics.

In the combustion process of an inhomogeneous combustible mixture, the degree of partial premixing affects various combustion stages differently, making it necessary to define each combustion stage clearly. Different combustion stages are determined based on combustion pressure signals in this study. The initial combustion duration $T_{initial}$ is defined as the interval from the ignition timing to the point when combustion pressure reaches 10% of the peak pressure. The main combustion duration T_{main} is defined as the interval during which combustion pressure rises from 10% to 90% of its peak value. The global combustion duration T_{peak} is the time required to reach the peak combustion pressure from the ignition timing. The combustion center of gravity $T_{gravity}$ is defined as the time required to reach 50% of the peak combustion pressure [47].

As the *MFT* decreases, the mixture in the combustion chamber has less time for component diffusion and turbulent dissipation, enhancing the degree of partial premixing. At this stage, high-concentration regions coexist with low-concentration regions in the combustion chamber, accompanied by flow field disturbances. Additionally, the flow field and concentration field continue to evolve due to turbulence dissipation and concentration diffusion, placing the mixture in a typical partially premixed state. This process is similar to the working environment of a gas fuel engine combustion chamber with in-cylinder direct injection technology. The effects of the degree of partial premixing and hydrogen content on the characteristic combustion durations of mixtures with different global equivalence ratios are shown in Figure 5.

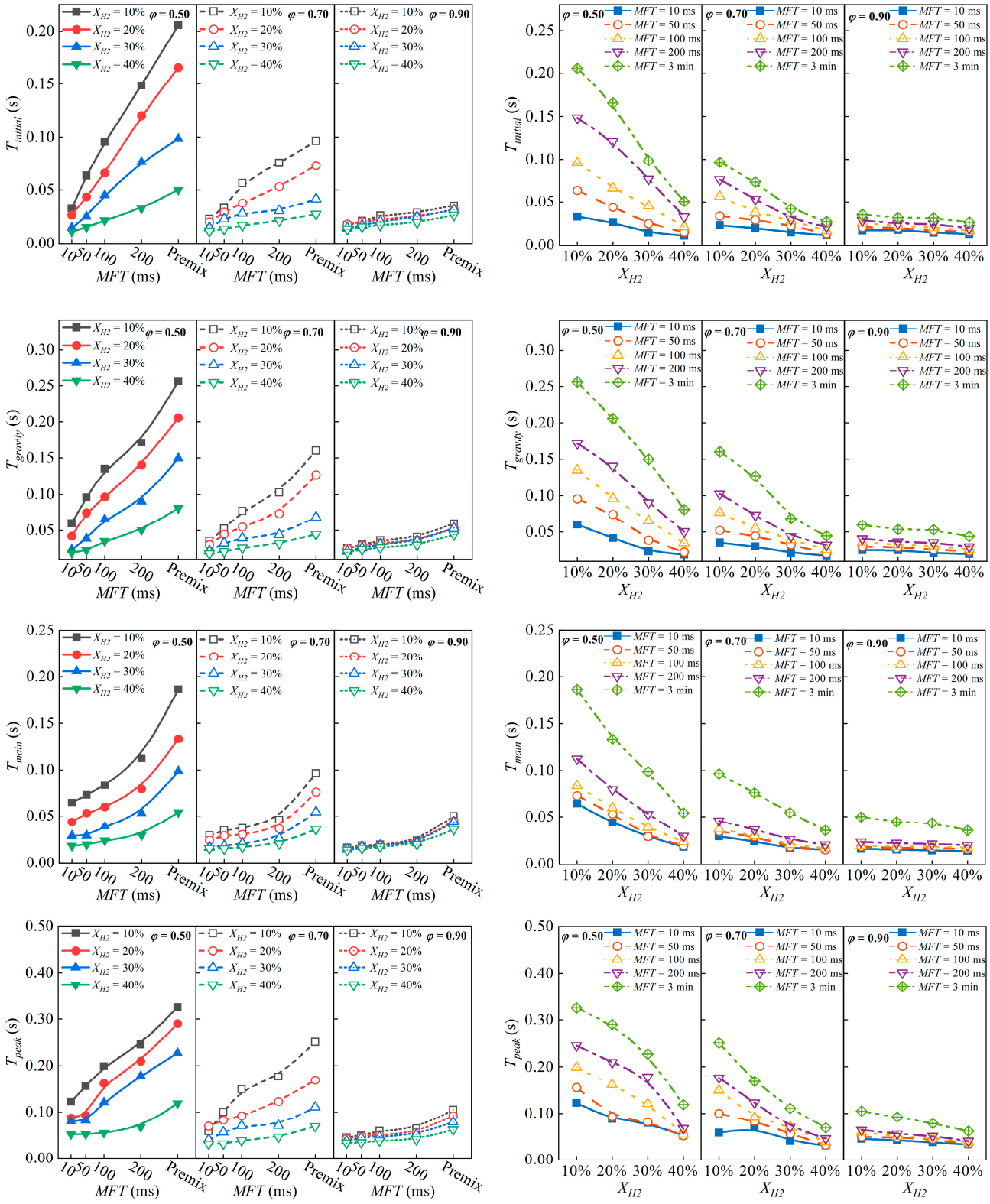


Figure 5. Effect of hydrogen content and partial premixing degree on characteristic combustion durations with different equivalent ratio mixtures.

When the global equivalence ratio and hydrogen content of the mixture remain constant, meaning the mixture composition in the CVCC remains unchanged, reducing the *MFT* enhances the degree of partial premixing, resulting in a continuous decrease in the characteristic combustion durations for different stages ($T_{initial}$, $T_{gravity}$, T_{main}, and T_{peak}). Compared to the homogeneous premixed combustion process, the partially premixed

non-homogeneous mixture can achieve rapid combustion. The main reasons are as follows: (1) back-support effect: the additional heat and species diffusion from the richer burned regions promote the chemical reaction mechanisms. (2) Enhanced transport by turbulence: turbulence disturbances enhance the transport processes and increase the collision probability of molecules, facilitating combustion reactions. (3) Non-homogeneous concentration and turbulence fields: The heterogeneous concentration and turbulence fields result in varying local flame fronts, increasing the flame front surface area and expanding the chemical reaction regions. This characteristic is also observed in methane–hydrogen–air mixtures with different equivalence ratios or hydrogen contents.

However, the influence of the partial premixing degree on the characteristic combustion durations varies with the mixture composition (equivalent ratio, hydrogen content). For partially premixed mixtures with the same equivalence ratio (hydrogen content), increasing the hydrogen content (equivalent ratio) in the mixture reduces the effect of the partial premixing degree on characteristic combustion durations. The main reason is that mixtures with a high equivalent ratio or high hydrogen content contain more active substances, which significantly increases the production rate of radicals (such as H, O, OH) in the combustion reaction chain, thereby accelerating the following elementary reaction processes: $H_2 + O \rightarrow OH + H$ and $H_2 + OH \rightarrow H + H_2O$. This enhances the propagation of chain chemical reactions and accelerates the decomposition of methane. Consequently, the overall combustion rate is significantly increased, rendering the influence of the partially premixed state relatively less significant.

In the partially premixed combustion process with the same *MFT*, meaning the degree of partial premixing is the same, increasing the hydrogen content in the mixture gradually shortens the characteristic combustion durations. Additionally, results show that hydrogen content has the most significant effect on promoting the premixed combustion process. This effect diminishes as the degree of partial premixing increases (i.e., as *MFT* shortens). At this point, the state of the mixture (inhomogeneous concentration field and strong turbulence field) plays a dominant role in influencing the combustion characteristic durations.

Reducing the *MFT* or increasing the hydrogen content in the mixture can both shorten the characteristic combustion durations and enable rapid combustion, with this promoting effect being more pronounced under the leaner combustion conditions. As the mixture concentration increases, this promoting effect gradually weakens. This is primarily due to the high concentration of reactive components that makes the combustion process predominantly governed by chemical kinetics, reducing the relative influence of turbulence mixing and local concentration stratification on the combustion rate.

The partially premixed combustion processes exhibit rapid combustion characteristics. These characteristics are jointly influenced by the mixture state (concentration field and turbulence field) and the reactivity of its components.

As shown in Figure 6, the peak combustion pressure trends are illustrated for partially premixed combustion processes with mixtures of different compositions. The enhancement of peak combustion pressure by the degree of partial premixing is relatively weak when the mixture's components remain constant. As the *MFT* decreases, the degree of partial premixing increases, enhancing the non-uniformity of combustion reactions in the mixture. This effect accelerates the heat release rate during the early combustion stage, resulting in a slight increase in combustion pressure. It is worth noting, however, that when the *MFT* becomes very short, the peak combustion pressure does not increase due to reduced heat loss; instead, it may even decrease slightly. The main reason is that the injected fuel has insufficient time to diffuse, causing parts of the mixture to exceed the flammability limits, leading to localized incomplete combustion and thereby limiting the further increase in pressure.

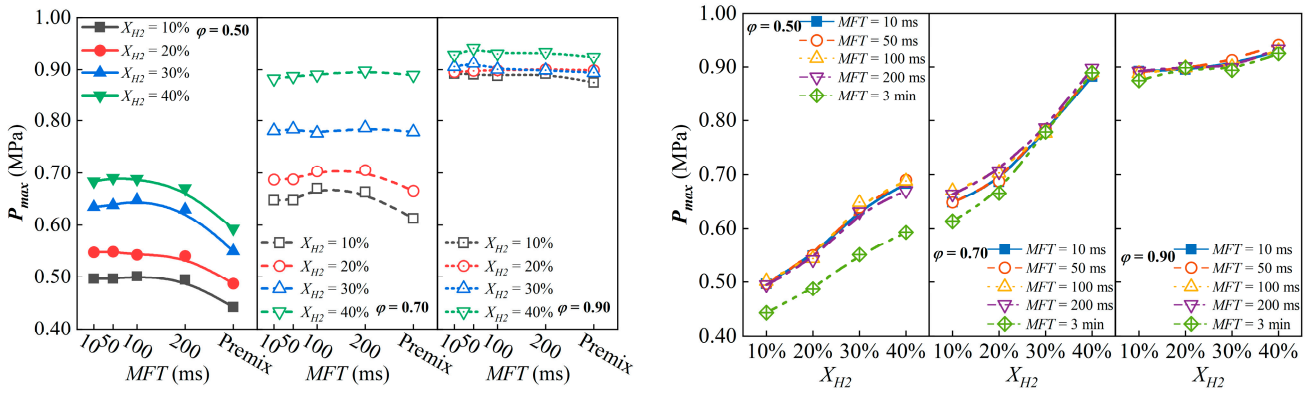


Figure 6. Effect of hydrogen content and partial premixing degree on combustion pressure peak with different equivalent ratio mixtures.

When the *MFT* remains constant, an increase in the equivalence ratio or hydrogen content leads to a continuous increase in the peak combustion pressure during the partially premixed combustion process, following a similar trend to that in homogeneous premixed combustion. The reason lies in the higher concentrations of reactive species (such as CH_4 and H_2) in mixtures with high equivalence ratios and high hydrogen content. These reactive species accelerate the production of radicals (H, O, OH), thereby enhancing the propagation rate of combustion reaction chains, speeding up the heat release process and ultimately driving higher combustion pressures. However, as the mixture equivalence ratio increases, the effect of hydrogen content on the peak pressure of partially premixed combustion weakens. This is because under high-equivalence-ratio conditions, the mixture is already rich in reactive combustion species. The additional contribution of hydrogen to the combustion rate diminishes as its marginal effect decreases.

3.2. Heat Release Characteristics of Partially Premixed Combustion

The heat release characteristics of the partially premixed combustion process were analyzed by processing and analyzing the combustion pressure signal using MATLAB R2021a. Due to the fast combustion rate and short duration of partially premixed combustion, heat transfer losses during the process are often neglected [48,49]. This study is conducted using a constant-volume combustion bomb platform, where the combustion chamber volume remains fixed. Consequently, the heat release rate is directly proportional to the pressure rise rate during combustion. The representative heat release rate (*RHRR*) [50] is calculated as

$$RHRR = \frac{dp}{dt} \tag{27}$$

The representative total heat release (*RTHR*) is obtained by integrating the representative heat release rate:

$$RTHR = \int_{t_{ignition}}^{t_{end}} RHRR dt \tag{28}$$

Here, $t_{ignition}$ and t_{end} represent the ignition start time and the combustion end time, respectively.

The normalized cumulative heat release rate (*NCHR*) provides a clear depiction of the combustion progress of partially premixed combustible mixtures under varying operating conditions. It is calculated as follows:

$$NCHR = \frac{\int_{t_{ignition}}^{t} RHRR dt}{RTHR} \tag{29}$$

Figure 7 illustrates the combustion characteristic parameter curves for premixed and partially premixed combustion processes, including combustion pressure p, burning velocity S_T, representative heat release rate $RHRR$, and normalized cumulative heat release rate $NCHR$. The combustion conditions are as follows: an equivalence ratio of 0.7, a hydrogen blending ratio of 20%, and mixture formation times of 100 ms (partially premixed combustion, solid line) and 3 min (premixed combustion, dashed line). In the premixed combustion process, the rise in combustion pressure is relatively gradual, with a relatively steady burning velocity and a lower heat release rate. During the 0.04–0.12 s combustion period, the burning velocity remains nearly constant. This phenomenon can be attributed to the uniform concentration distribution of the mixture in premixed combustion, where the combustion reaction is primarily governed by chemical reaction kinetics, resulting in a relatively low and stable flame propagation speed. When the MFT is shortened, the combustible mixture transitions to a partially premixed state, exhibiting significantly different combustion characteristics. Under this condition, the mixture concentration within the combustion chamber becomes inhomogeneous, with higher concentrations near the ignition electrode at the chamber's center and lower concentrations near the combustion bomb wall. The presence of this concentration gradient significantly enhances combustion reactions in locally fuel-rich regions, particularly in the central area where the concentration and turbulence intensity near the spark plug are higher, accelerating the propagation of combustion chain reactions. The fuel injection dynamics further amplify the turbulence effects, leading to a substantial increase in flame propagation speed and heat release rate. Compared to premixed combustion, the heat release rate curve of partially premixed combustion exhibits a rapid rise to a peak followed by a sharp decline, forming a distinct single-peak profile. This rapid heat release directly drives a rapid increase in combustion pressure while shortening the combustion duration. The burning velocity and the representative heat release rate curve exhibit similar variation patterns. Due to the identical composition of the combustible mixture, the peak combustion pressures in premixed and partially premixed combustion processes are comparable. This is because the combustible mixture composition in both combustion processes is identical, resulting in a similar total heat release amount that determines the peak combustion pressure. However, due to the higher combustion reaction rate in partially premixed combustion, the heat release process is more concentrated in the early combustion stage, leading to a significantly higher pressure rise rate compared to premixed combustion.

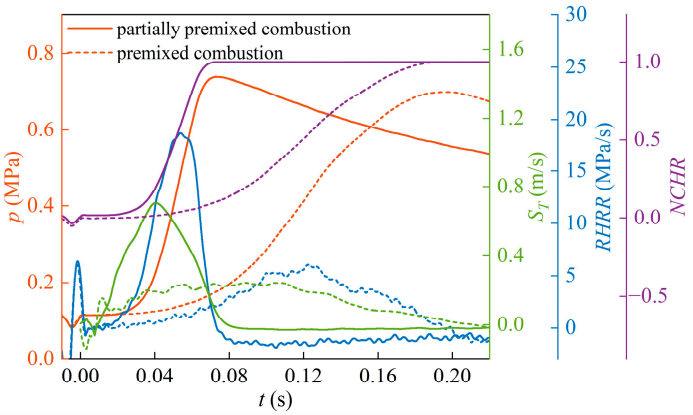


Figure 7. Characterization of premixed and partially premixed combustion processes.

Figure 8 illustrates the impact of the partial premixing degree on the peak representative heat release rate $RHRR_{max}$ and its timing $T - RHRR_{max}$ under various conditions. As the MFT decreases, the degree of partial premixing increases, resulting in a higher $RHRR_{max}$ and an earlier $T - RHRR_{max}$. This trend is observed across combustion pro-

cesses with different equivalence ratios or hydrogen contents. This indicates that the degree of partial premixing has a general enhancing effect on the heat release rate and the dynamic characteristics of the heat release process. For mixtures with the same global equivalence ratio but varying hydrogen content, the effect of the partial premixing degree on the $RHRR_{max}$ remains similar (have similar slope), while its influence on the $T - RHRR_{max}$ gradually weakens with hydrogen content increases. This is because in high-hydrogen-content mixtures, the combustion reaction rate is primarily governed by the chemical properties of hydrogen, while the marginal impact of turbulent mixing and concentration non-uniformity on heat release is relatively low. Under the same MFT, the $RHRR_{max}$ increases with higher hydrogen content. The high diffusivity and low ignition energy of hydrogen significantly enhance localized combustion reactions, thereby accelerating the heat release rate and advancing the occurrence time of the peak heat release rate. The effect of hydrogen content on the $RHRR_{max}$ of partially premixed combustion is most significant for mixtures with an equivalence ratio of 0.7.

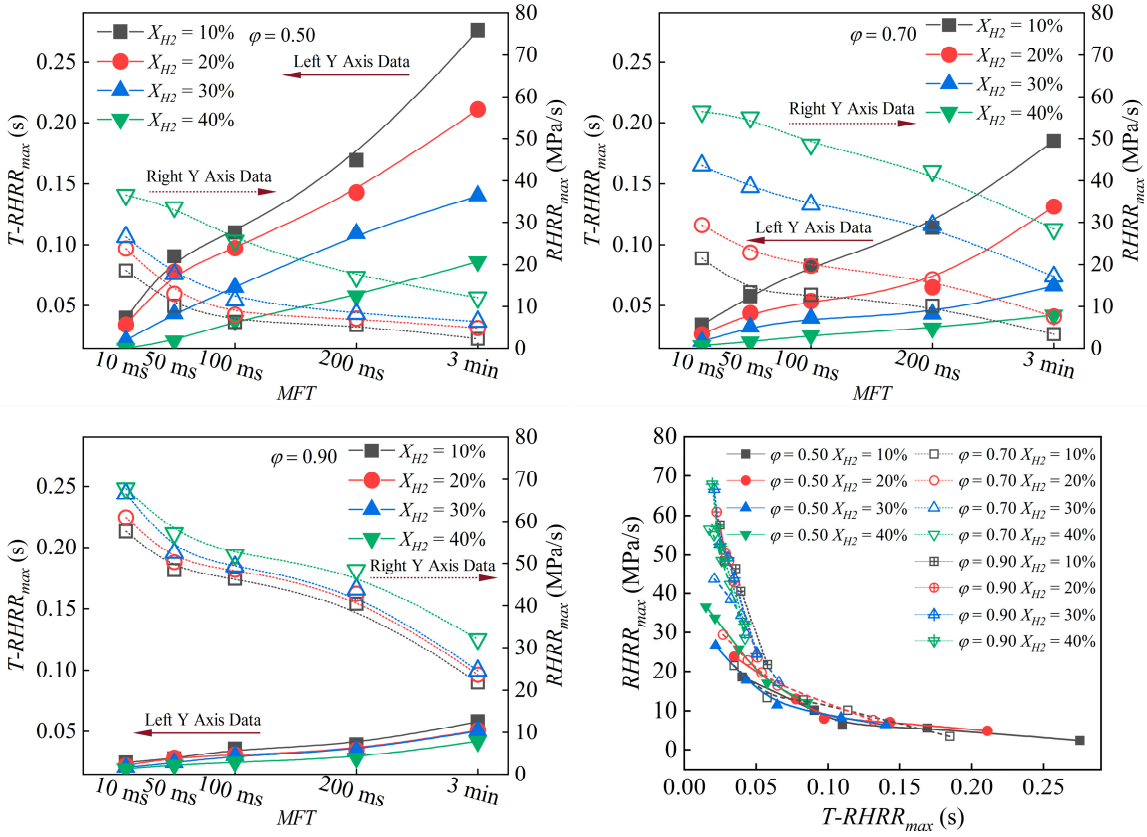


Figure 8. Effects of the partial premixing degree on the representative heat release rate peaks $RHRR_{max}$ and peak moments $T - RHRR_{max}$.

In contrast, its influence is weaker for leaner (equivalence ratio of 0.5) or richer (equivalence ratio of 0.9) mixtures. This is mainly because a lean mixture (equivalence ratio of 0.5) is affected by the limited fuel supply, which restricts the availability of reactive species in the combustion reaction. Even with an increase in hydrogen content, its enhancement effect on the heat release rate is limited, making it difficult to significantly improve the heat release process. For rich mixtures (equivalence ratio of 0.9), under higher-equivalence-ratio conditions, the concentration of fuel components in the mixture is higher, and the combustion reaction and heat release process may be dominated by the high chemical reaction rate.

Figure 9 shows the normalized cumulative heat release rate curves under various operating conditions. For mixtures with the same composition (equivalence ratio and hydrogen content), a shorter *MFT* leads to a higher degree of partial premixing. Consequently, the *NCHR* at the same time point increases, the overall combustion rate accelerates, and the combustion duration shortens. Two primary factors contribute to this phenomenon, namely (1) flow field disturbance from fuel injection: The disturbances in the flow field caused by fuel injection accelerate the transport of materials along the flame front. This creates wrinkles on the flame front, increasing its surface area, expanding the chemical reaction zone, and enhancing heat release [51]. (2) Back-support effect of locally stratified mixtures: As the flame propagates from high-concentration to low-concentration regions, active species and heat are transferred to unburned areas through gradient effects, promoting the heat release process during combustion [52]. As the hydrogen content or equivalent ratio in the mixture increases, the promotion effect of the partial premixing degree on heat release weakens. Under high-hydrogen-content conditions, the combustion process is primarily controlled by the chemical reaction rate of hydrogen. Under high-equivalence-ratio conditions, the higher fuel concentration leads to the combustion reaction rate being dominated by the high reactivity of the fuel, while the influence of the partial premixing degree (turbulence effects or concentration gradients) on heat release becomes relatively weaker. At lower degrees of partial premixing, the equivalence ratio and hydrogen content of the mixture have a more pronounced influence on *NCHR*. The results show that the degree of partial premixing, hydrogen content, and equivalence ratio have a synergistic influence on the dynamic changes in *NCHR*.

3.3. Partially Premixed Burning Velocity S_T

Shortening the *MFT* leads to an inhomogeneous concentration distribution of the mixture within the combustion chamber accompanied by flow field disturbances, at which point the burning velocity of the partially premixed mixture is constantly changing. Figure 10 shows the variation in burning velocity with combustion time under different operating conditions. For mixtures with different compositions, the burning velocity curve has a similar trend to the heat release rate curve, showing a rapid rise to a maximum value followed by a relatively slower decrease. This is because, in this study, central ignition is used. During the initial combustion phase, the flow field near the spark plug is relatively strong and the mixture concentration is higher, leading to a rapid increase in the burning velocity, which reaches its peak. As the flame propagates from the central region toward the chamber walls, the flow field disturbances gradually weaken and the mixture concentration becomes more diluted, causing the burning velocity to decrease. During the later stages of combustion, flame propagation is constrained by the structure and walls of the combustion chamber. This geometric confinement inhibits the further development of the flame front, while wall effects increase heat loss, thereby reducing the burning velocity until the combustion process is complete.

For the premixed combustion process (*MFT* = 3 min), the burning velocity remains constant for a period of time while the flame is in a relatively stable development phase. In the case of partially premixed combustion, as the *MFT* decreases, the burning velocity increases and the global combustion duration shortens. The duration of the relatively stable development phase gradually decreases and may even disappear. This indicates that the dynamic process of flame propagation is more influenced by the initial turbulence and concentration distribution. As the *MFT* shortens, the peak moment of burning velocity also moves forward. The primary reasons for this are as follows: (1) the enhancement of initial flow field disturbances; (2) the acceleration effect in locally fuel-rich regions; and (3) the

non-uniformity of flame propagation. The *MFT* has a greater effect on the early stages of the combustion process.

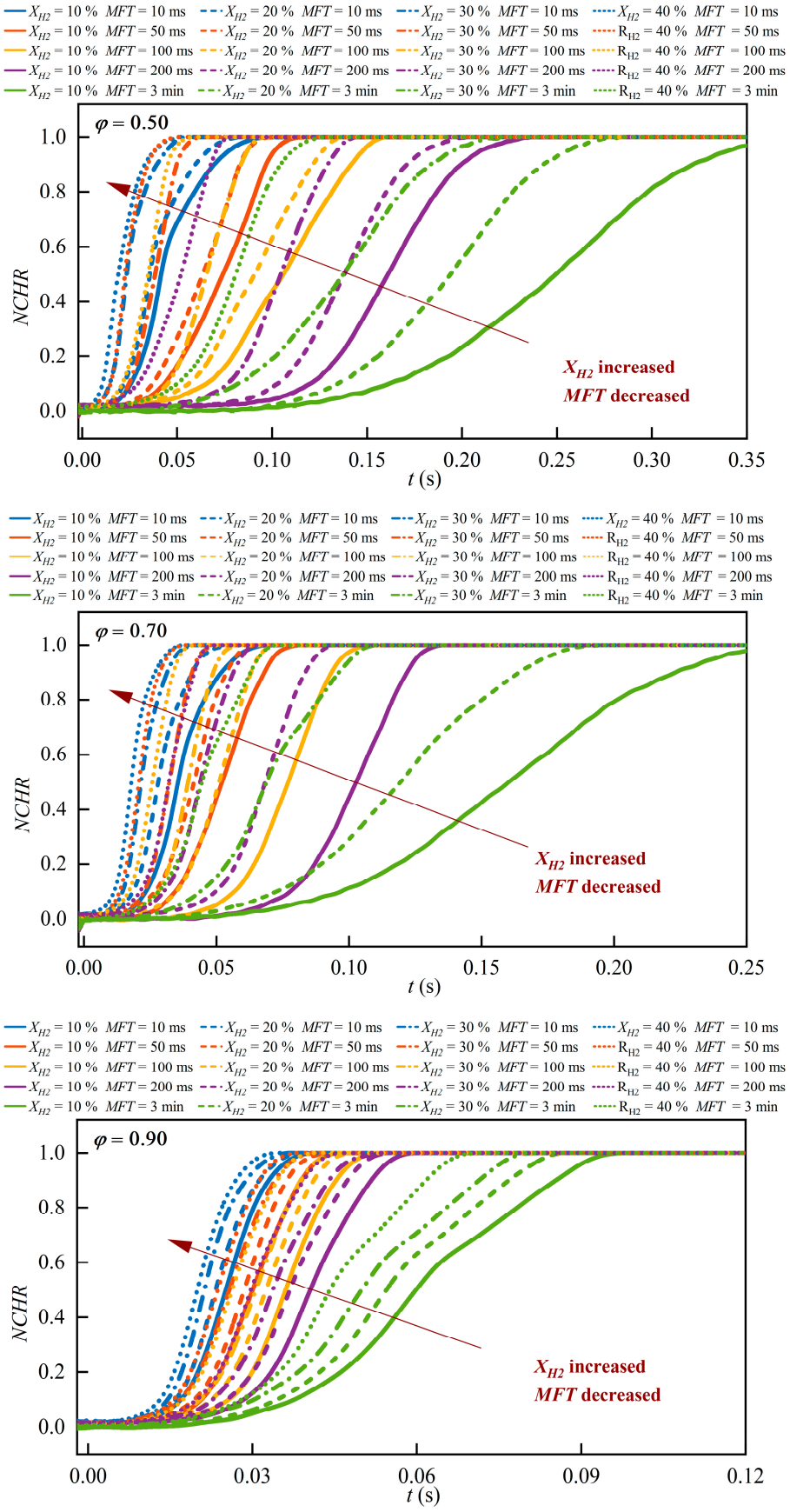


Figure 9. Normalized cumulative heat release rate under different operating conditions.

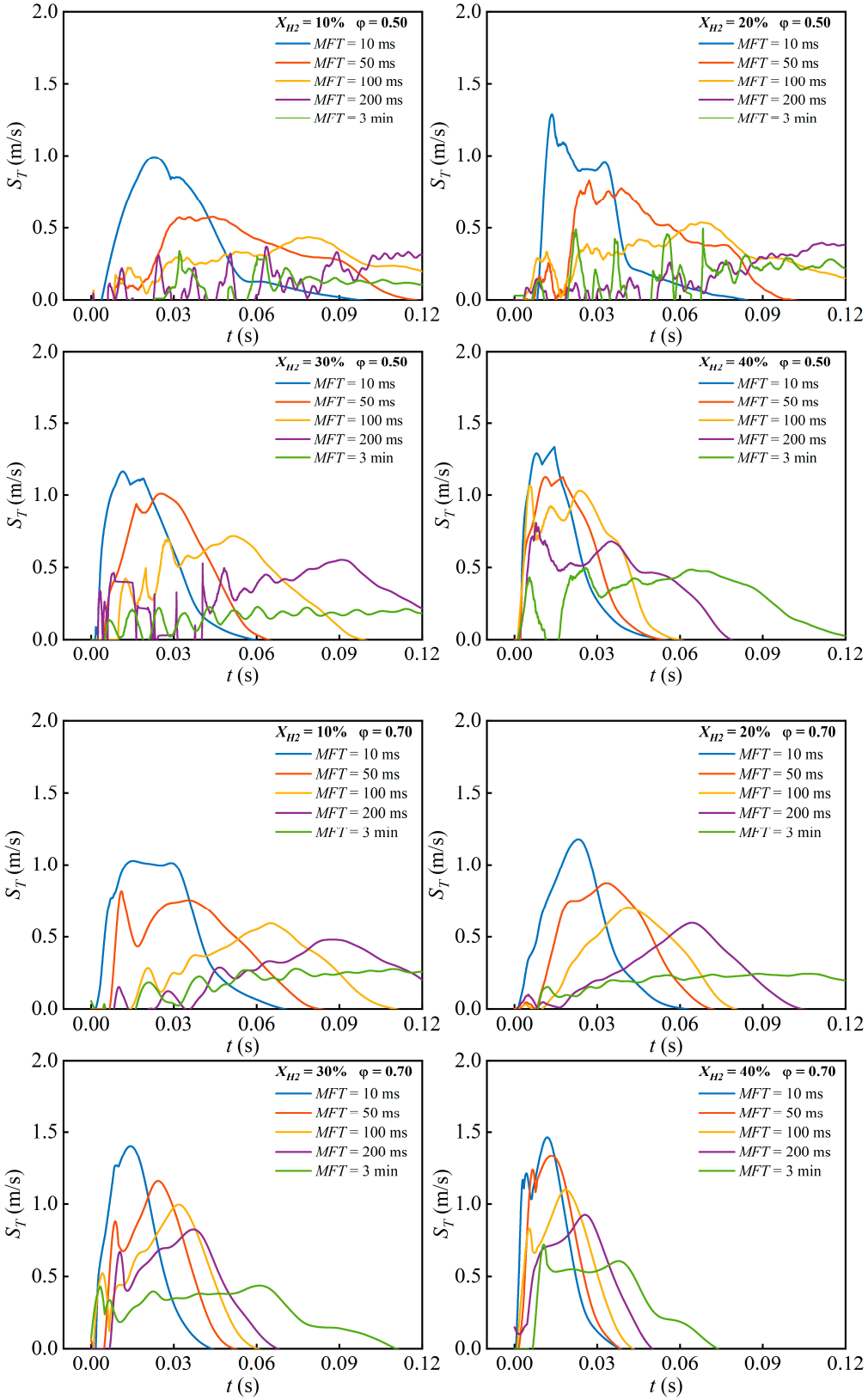


Figure 10. *Cont.*

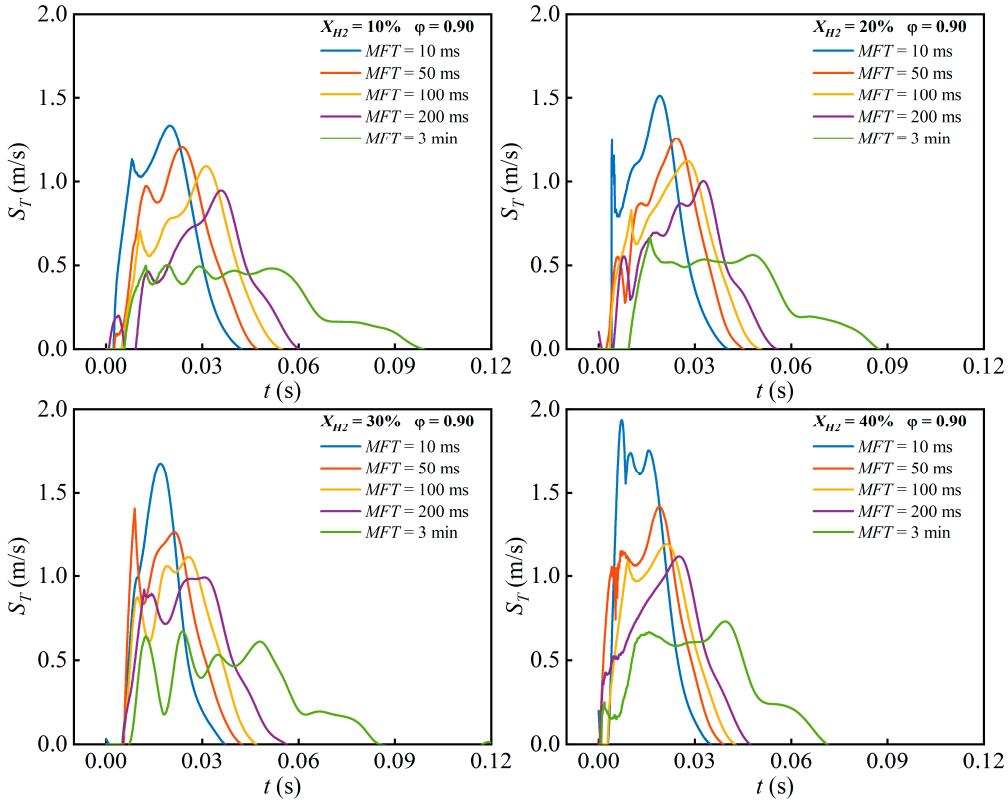


Figure 10. Burning velocity curves for partially premixed combustion processes with different equivalence ratios and hydrogen contents.

As the equivalence ratio or hydrogen content in the mixture increases, the burning velocity continually increases. This is because high equivalence ratios and high hydrogen content significantly enhance the chemical reactivity of the mixture, accelerating the propagation of chain reactions by generating more radicals (H, OH, O), thereby increasing the burning velocity. However, for combustible mixtures with different equivalence ratios or hydrogen contents, the combustion process of partially premixed combustion follows a similar evolutionary trend.

The peak burning velocities $S_{T\text{-}max}$ and their corresponding timings $T - S_{T\text{-}max}$ under different operating conditions are shown in Figure 11. For mixtures with the same composition, as the *MFT* decreases and the degree of partial premixing increases, the $S_{T\text{-}max}$ increases, and the $T - S_{T\text{-}max}$ occurs earlier. This trend indicates that under shorter *MFT* conditions, the concentration distribution of the mixture is more uneven, the chemical reaction rate in locally fuel-rich regions is higher, and the flow field disturbances are stronger. These combined effects significantly accelerate the flame propagation speed, causing the moment when the combustion rate reaches its peak to occur much earlier. As the hydrogen content or equivalence ratio of the mixture increases, the reactivity of the mixture increases, leading to faster combustion, an earlier $T - S_{T\text{-}max}$, and a higher $S_{T\text{-}max}$. Hydrogen's high diffusivity and chemical reactivity accelerate the propagation of combustion chain reactions by enhancing the generation rate of radicals (H, OH, O), while a higher equivalence ratio increases the energy density of the mixture, leading to greater heat release during combustion. These factors jointly contribute to the increase in burning velocity and significantly shorten the combustion duration. For mixtures with different equivalence ratios or hydrogen contents, the $S_{T\text{-}max}$ and $T - S_{T\text{-}max}$ follow a similar nonlinear trend. There is consistency with the pattern of change in the peak heat release rate and the peak moment shown in Figure 8. In the slower combustion cases, where the combustion rate is slower and the combustion duration is longer, such as for combustible mixtures with low equiva-

lence ratios and low hydrogen content, the state of the combustible mixture (concentration field and turbulence field) has a significant impact on the combustion process. The flame propagation is more dependent on local concentration gradients and turbulent mixing effects. As the mixture reactivity increases (due to a higher equivalence ratio or hydrogen content), the combustion process becomes more dominated by chemical reaction kinetics, and the influence of turbulence and concentration field non-uniformity on the combustion reaction rate diminishes.

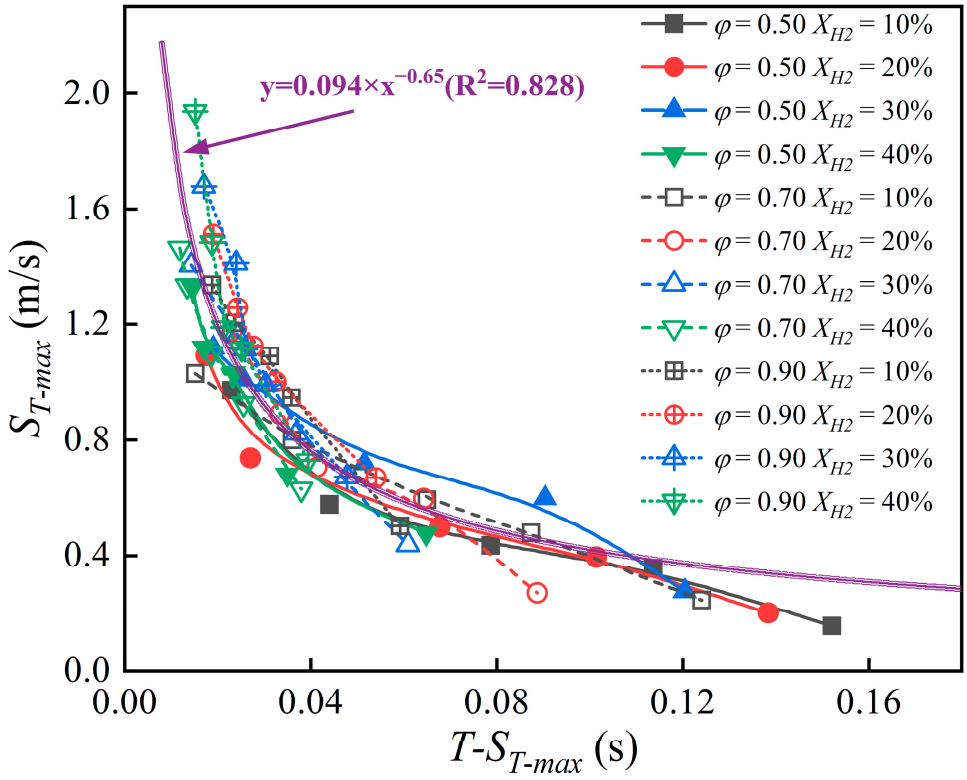


Figure 11. Peak $S_{T\text{-}max}$ and peak moment $T - S_{T\text{-}max}$ of partially premixed burning velocity under different operating conditions.

The combustion duration of combustible mixtures with varying degrees of partial premixing differs significantly. Even at the same moment in time, the combustion processes may be at different stages. To better compare the evolution and differences in burning velocity across identical combustion stages, it is necessary to synchronize the combustion progress.

Nagy et al. [53] proposed a relationship between burning velocity S_T and the temperature and pressure of the mixture, which can be used to calculate the initial burning velocity S_T^i:

$$S_T = S_T^i \left(\frac{T_b}{T_i}\right)^{\alpha} \left(\frac{p}{p_i}\right)^{\beta} = S_T^i \left(\frac{p}{p_i}\right)^{\alpha((\gamma_u - 1)/\gamma_u) + \beta} \tag{30}$$

where α and β are the thermal and pressure coefficients, respectively, determined empirically.

This equation indicates a correlation between burning velocity and the pressure ratio p/p_i. Mixtures with the same composition but varying degrees of partial premixing exhibit relatively similar peak combustion pressures. In this study, using the pressure ratio p/p_i to synchronize combustion progress is a reliable approach.

The effect of partial premixing on burning velocity during identical combustion stages under varying operating conditions is a critical area of study. Figure 12 illustrates the relationship between burning velocity and the pressure ratio. For methane–hydrogen–air partially premixed combustion, the enhancement of burning velocity due to partial premixing is most pronounced during the low-pressure-ratio stage, corresponding to the early combustion phase. This is primarily due to the stronger flow field disturbances and greater concentration non-uniformity during the early combustion stage. Under partial premixing conditions, the heat release rate in locally fuel-rich regions is significantly enhanced, thereby accelerating flame propagation and the combustion reaction rate. For mixtures with the same composition, as the pressure ratio increases, differences in burning velocity across varying degrees of partial premixing diminish. In the later stages of combustion, as the combustible mixture is gradually consumed, flame propagation becomes constrained by wall effects and heat losses. The burning velocities of mixtures with different partial premixing levels converge, and the influence of partial premixing becomes negligible. As the *MFT* decreases, the peak burning velocity occurs earlier, shifting the combustion enhancement effect to an earlier phase. This trend is consistent across mixtures with varying equivalence ratios and hydrogen content. However, with higher equivalence ratios or hydrogen content, high equivalence ratios and hydrogen content accelerate chain reaction propagation, enhancing the overall combustion reaction rate, and the impact of partial premixing on burning velocity becomes more significant during the low-pressure-ratio stage.

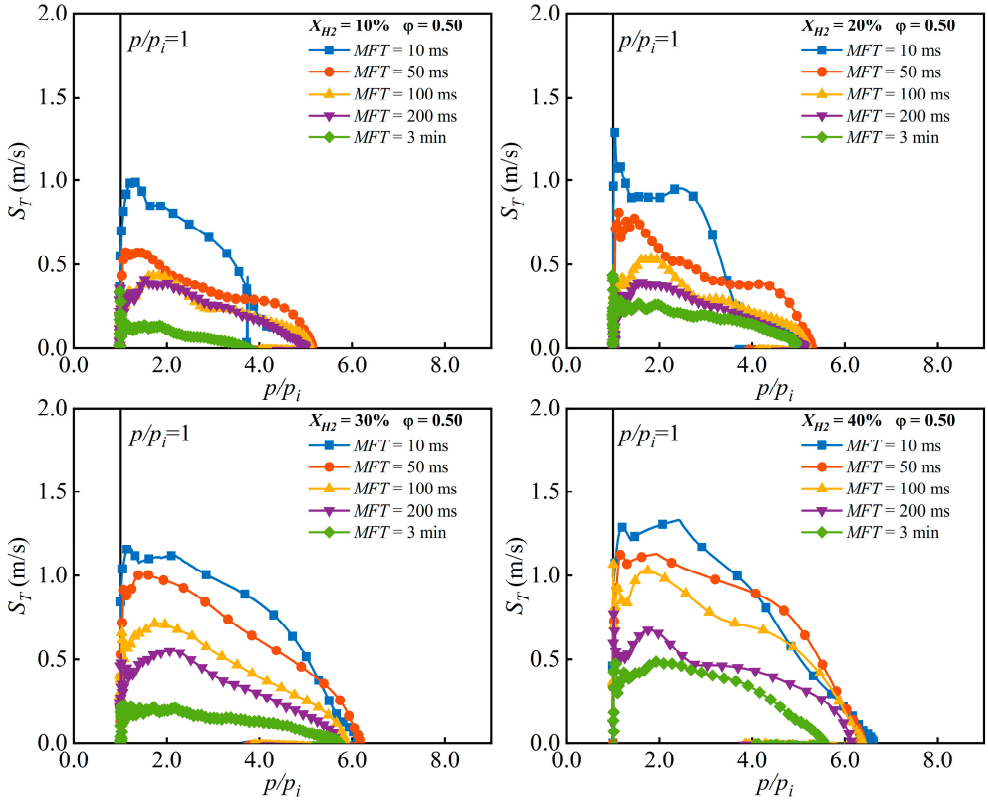


Figure 12. *Cont.*

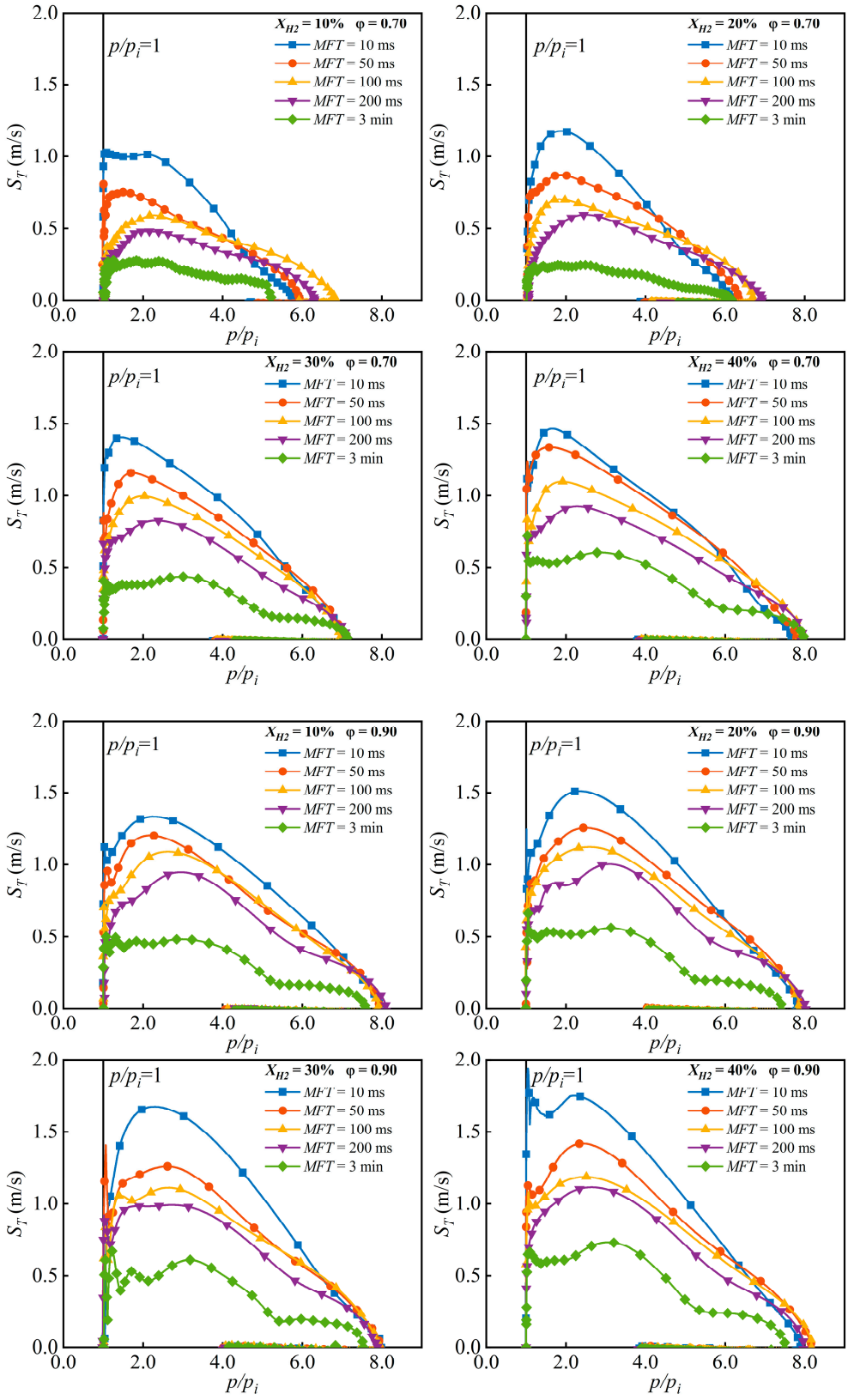


Figure 12. Partially premixed burning velocity vs. pressure ratio.

3.4. Effects of Equivalence Ratio, Hydrogen Content, and Partial Premixing Degree

For the partially premixed combustion process, the peak burning velocity $S_{T\text{-}max}$ and the timing of the peak $T - S_{T\text{-}max}$ are important characteristic parameters for evaluating the combustion process. The $S_{T\text{-}max}$ reflects the maximum intensity of the burning velocity

of the mixture, while the $T - S_{T\text{-}max}$ indicates the time point at which the burning velocity reaches its maximum. These parameters directly affect combustion efficiency, heat release characteristics, and combustion stability.

The $S_{T\text{-}max}$ values under different operating conditions are shown in Figure 13. The $S_{T\text{-}max}$ is significantly affected by the degree of partial premixing (*MFT*). As the *MFT* increases, the degree of partial premixing decreases and the mixture state becomes more stable and homogeneous. This reduces the localized intensification effect of the combustion reaction, leading to a gradual decrease in the $S_{T\text{-}max}$. This trend is observed for combustible mixtures with different compositions. As the hydrogen content increases, the impact of *MFT* on the $S_{T\text{-}max}$ becomes more pronounced (the curve becomes steeper). The occurrence of this phenomenon can be attributed to the following reasons: (1) enhanced local combustion reactions due to hydrogen's preferential diffusion effect: Hydrogen molecules possess a high diffusion coefficient, exhibiting significant preferential diffusion characteristics in non-uniform mixtures. As the degree of partial premixing increases, hydrogen more easily diffuses into regions with lower local concentrations, forming highly reactive combustion zones that significantly increase the burning velocity. This preferential diffusion effect becomes more pronounced with higher hydrogen content, leading to a greater sensitivity of the $S_{T\text{-}max}$. (2) Strengthening of chemical reaction chains: Hydrogen effectively generates reactive radicals (H, OH, O), accelerating the propagation of chain reactions and enhancing the overall reaction rate of the mixture. Under partially premixed conditions, this chain reaction enhancement effect, coupled with turbulent mixing effects, results in a significant increase in the $S_{T\text{-}max}$ as hydrogen content rises. These combined effects explain the observed relationship between hydrogen content and combustion dynamics.

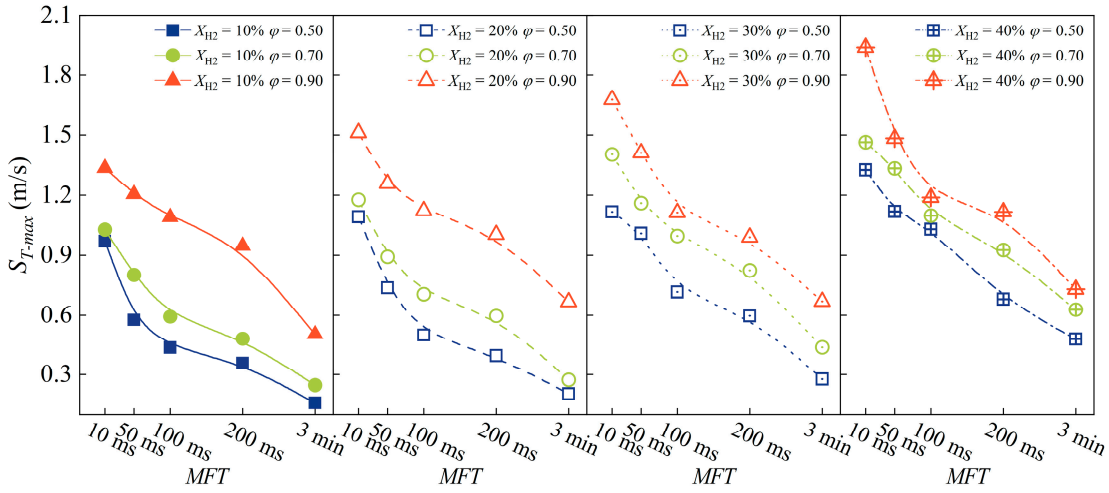


Figure 13. Effects of the partial premixing degree on the burning velocity peaks $S_{T\text{-}max}$ with different equivalence ratios and hydrogen content mixtures.

Additionally, as the hydrogen content increases, the $S_{T\text{-}max}$ differences between different equivalence ratios gradually diminish. This is because in high-hydrogen-content mixtures, the combustion reaction rate is primarily governed by the chemical reactivity of hydrogen. The influence of the equivalence ratio on burning velocity is diminished by hydrogen's preferential diffusion and chain reaction enhancement effects.

To investigate the impact of various factors on the enhancement of $S_{T\text{-}max}$ during the partially premixed combustion process (compared to premixed combustion), the "relative peak burning velocity $R - S_{T\text{-}max}$" is defined as the ratio of the peak burning velocity under partially premixed conditions to that under premixed conditions for the same mixture composition.

As shown in Figure 14, the $R-S_{T\text{-}max}$ under different operating conditions varies. As the *MFT* decreases, the degree of partial premixing increases, resulting in the formation of locally fuel-rich regions, which enhance the local combustion reaction rate. Simultaneously, the increased turbulence intensity strengthens the flame propagation process, further promoting the increase in burning velocity. This effect is most pronounced at an equivalence ratio of 0.5 and diminishes as the equivalence ratio increases.

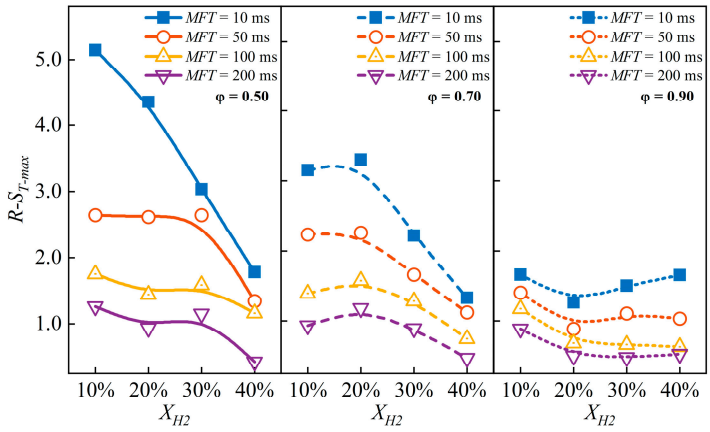


Figure 14. The promotion of the partial premixing degree on the relative burning velocity peaks $R-S_{T\text{-}max}$ with different equivalence ratios and hydrogen content mixtures.

Hydrogen content has a significant effect on burning velocity. When hydrogen content is lower, there is a significant difference in the $R-S_{T\text{-}max}$ across different mixture formation times. For mixtures with the same equivalence ratio and degree of partial premixing, an increase in hydrogen content leads to a gradual decrease in the $R-S_{T\text{-}max}$. This occurs because at low hydrogen contents, the combustion reaction rate of the mixture is primarily influenced by local concentration non-uniformities and turbulence intensity. However, as hydrogen content increases, the concentration of reactive species in the mixture increases, causing the combustion reaction rate to gradually approach saturation, and the combustion reactions become increasingly dominated by the chemical properties of hydrogen.

In addition, hydrogen's high reactivity and diffusivity, combined with its preferential diffusion effect, allow the increased degree of partial premixing to further enhance the local concentration advantage of hydrogen in the mixture, thereby significantly increasing the combustion rate. Under high-equivalence-ratio conditions, the combustion reaction becomes dominated by overall chemical kinetics, and the relative contribution of hydrogen diffusion gradually diminishes.

In order to better characterize the burning velocity characteristics of partially premixed combustion, the "relative peak burning velocity timing $T-S_{T\text{-}max}/T_{peak}$" is defined as the ratio of the peak burning velocity timing $T-S_{T\text{-}max}$ to the global combustion duration T_{peak}. This parameter reflects the relative position of the $S_{T\text{-}max}$ during the combustion process and serves as an important indicator for evaluating the dynamic characteristics of combustion.

Figure 15 shows the $T-S_{T\text{-}max}/T_{peak}$ under various operating conditions. For partially premixed combustion processes with different compositions, as the *MFT* decreases and the degree of partial premixing increases, the $T-S_{T\text{-}max}/T_{peak}$ decreases, causing the peak burning velocity to occur earlier. This indicates that the $S_{T\text{-}max}$ occurs earlier relative to the overall combustion process. The reason lies in the fact that a shorter *MFT* results in a more stratified concentration distribution of the mixture and enhanced flow field disturbances, leading to a more concentrated combustion reaction during the early stages. Particularly in

locally fuel-rich regions, the nonlinear increase in reaction rates accelerates the heat release process, causing the $S_{T\text{-}max}$ to appear earlier.

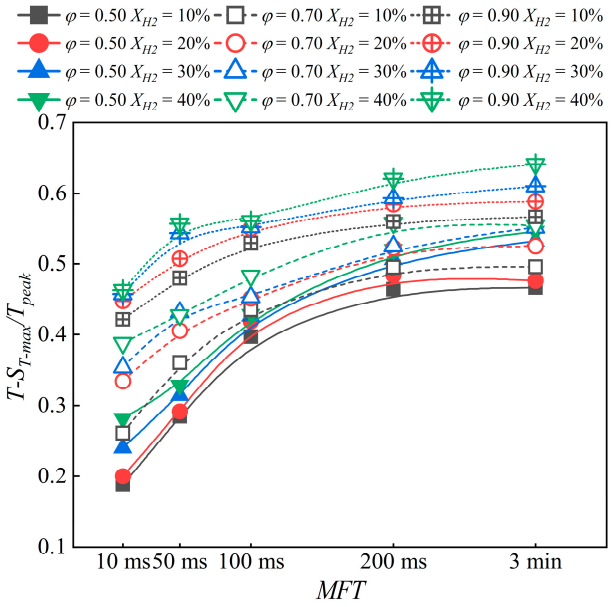


Figure 15. Effects of partial premixing degree on the relative burning velocity peak moment $T - S_{T\text{-max}}/T_{peak}$ with different equivalence ratios and hydrogen content mixtures.

As the *MFT* shortens, the effect of the mixture composition on the $T - S_{T\text{-}max}/T_{peak}$ gradually becomes more significant. This is because the non-uniformity of the concentration field and turbulence field further intensifies the localized combustion reactions. When the equivalence ratio or hydrogen content in the mixture is lower, the combustion rate is more dependent on local concentration gradients and turbulent mixing effects, making the impact of *MFT* variations on the dynamic characteristics of combustion particularly significant. Under conditions of constant *MFT*, the $T - S_{T\text{-}max}/T_{peak}$ increases as the equivalence ratio or hydrogen content in the mixture increases. The *MFT* has a large impact on the $T - S_{T\text{-}max}/T_{peak}$; however, as the reactivity of the mixture components increases, this effect diminishes. This is because at this stage, the combustion rate is primarily governed by reaction kinetics, while the effects of the flow field and concentration field become relatively minor.

3.5. Correlation Between Partially Premixed Burning Velocity and Combustion Pressure

During the combustion process of a combustible mixture, the combustion pressure continuously increases with the rise in heat release. The burning velocity of the mixture significantly influences the pressure curve of the combustion process. The burning velocity S_T, combustion pressure p, first-order derivative dp/dt, and second-order derivative d^2p/dt^2 of pressure for the partially premixed combustion process with a hydrogen content of 20%, equivalence ratio of 0.7, and *MFT* of 100 ms are shown in Figure 16. The peak moment of the partially premixed burning velocity $T - S_{T\text{-max}}$ occurs almost simultaneously with the peak moment of the second-order derivative of the combustion pressure $T - (d^2p/dt^2)_{\max}$. This indicates a high degree of synchronization between the rapid increase in burning velocity and the accelerated rise in combustion pressure. This phenomenon is consistent with that in turbulent premixed combustion [34]. Mechanistically, during the early stages of flame propagation, the chemical reaction rate of the mixture increases sharply, significantly enhancing the heat release. This, in turn, causes the acceleration of combustion pressure (i.e., the second derivative) to reach its peak rapidly. When the combustion pressure reaches its maximum value, the partially premixed burning velocity decreases to zero. At the

moment, the combustible mixture in the combustion chamber is nearly depleted, and the flame propagation speed subsequently decreases. At this stage, the pressure variation in the combustion chamber is primarily governed by the combined effects of residual heat release and wall heat losses. The peak of the partially premixed burning velocity occurs in the early stages of the global combustion process, in agreement with the results of Figure 12.

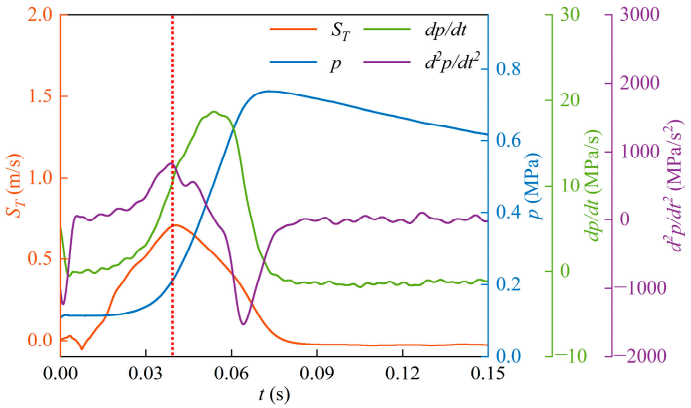


Figure 16. The correlation between the burning velocity S_T, pressure p, first-order derivative of pressure dp/dt, and second-order derivative of pressure d^2p/dt^2. (The red dotted line: the maximum values of S_T and d^2p/dt^2 occur at the same time.)

Additionally, the dynamic relationship between combustion pressure and burning velocity reveals a clear coupling characteristic across different stages of the combustion process. Changes in the burning velocity directly affect the heat release rate, which in turn determines the magnitude and rate of increase in combustion pressure.

The correspondence between the peak moment of the burning velocity $T - S_{T\text{-max}}$ and the peak moment of the second-order derivative of the combustion pressure $T - (d^2p/dt^2)_{\max}$ for the partially premixed combustion process under different operating conditions is shown in Figure 17a. With equivalence ratio or hydrogen content in the combustible mixture increasing or the *MFT* being shortened, the combustion process is accelerated and $T - S_{T\text{-max}}$ is constantly advancing. At the same time, the combustion duration is shortened and $T - (d^2p/dt^2)_{\max}$ is also advancing. $T - S_{T\text{-max}}$ and $T - (d^2p/dt^2)_{\max}$ almost always occur at the same time for partially premixed combustion processes under different operating conditions. This phenomenon indicates that changes in the combustion rate directly drive the dynamic behavior of combustion pressure. Furthermore, this trend remains consistent under different operating conditions and is not significantly affected by mixture composition (e.g., equivalence ratio and hydrogen content) or mixture state (e.g., flow field intensity and concentration gradients).

The correlation between the peak of the second-order derivative of the combustion pressure $(d^2p/dt^2)_{\max}$ and the peak of the partially premixed burning velocity $S_{T\text{-max}}$ is further explored, as shown in Figure 17b. With the increase in the equivalence ratio and hydrogen content in the combustible mixture or the shortening of *MFT*, the combustion pressure increases, $(d^2p/dt^2)_{\max}$ keeps increasing, and $S_{T\text{-max}}$ also keeps increasing, but it does not show a linear correlation. When the equivalence ratio or hydrogen content in the mixture is lower, $S_{T\text{-max}}$ exhibits a rapid change in response to $(d^2p/dt^2)_{\max}$, indicating that the combustion process is more significantly influenced by the state of the mixture. Conversely, when the equivalence ratio or hydrogen content in the mixture is high, the combustion reaction rate tends to saturate due to the abundance of reactive species in the mixture, leading to a slower response to $(d^2p/dt^2)_{\max}$. As the equivalence ratio increases, this trend diminishes. This phenomenon is caused by the interaction of mixture components, turbulent flow field, and concentration field.

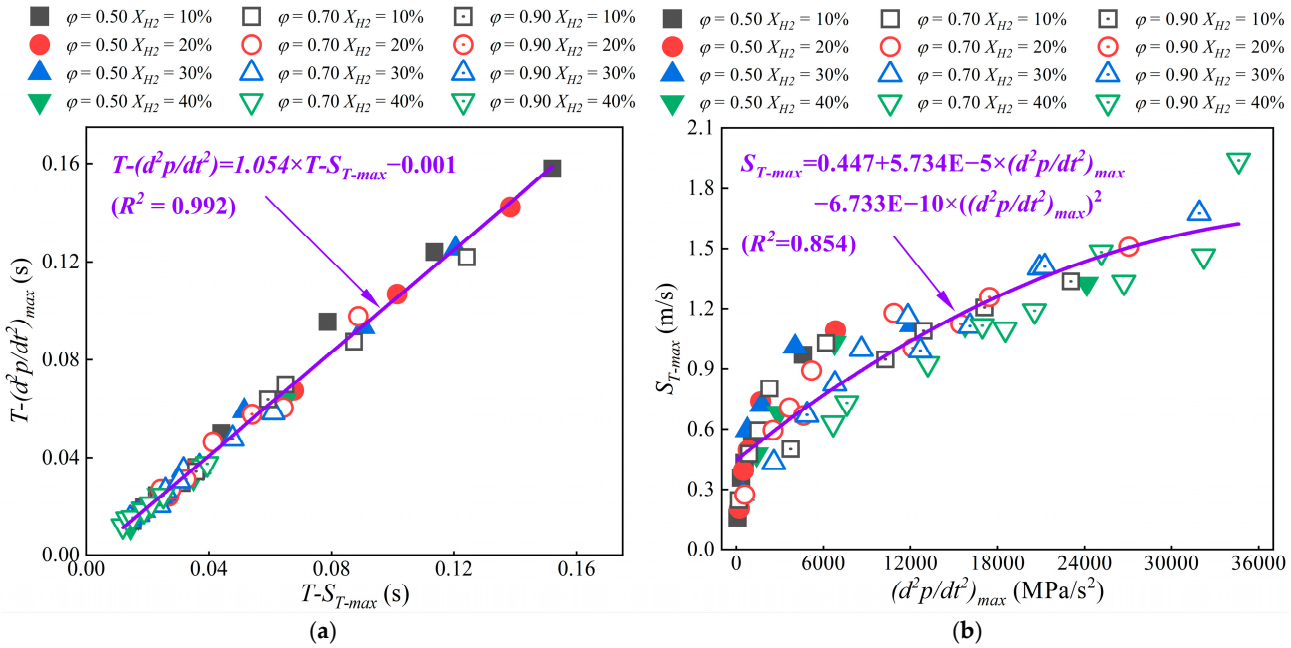


Figure 17. (**a**) Correlation between the peak moments of burning velocity $T - S_{T\text{-max}}$ and the peak moments of the second-order derivative of combustion pressure $T - (d^2p/dt^2)_{\max}$ under different operating conditions. (**b**) Correlation between the peak values of burning velocity $S_{T\text{-max}}$ and the peak values of the second-order derivative of combustion pressure $(d^2p/dt^2)_{\max}$ under different operating conditions.

4. Conclusions

Controlling the concentration distribution of combustible mixtures to achieve partially premixed combustion is an efficient way to accelerate the combustion process and improve ICE performance. However, under the influence of inhomogeneous concentration fields and disturbed flow fields, the combustion behavior of partially premixed mixtures in a confined space is complex, particularly under different partial premixing degrees and mixture compositions. In this paper, experiments on the partially premixed combustion of methane–hydrogen–air mixtures were conducted on a constant-volume combustion bomb experimental platform. The effects of the degree of partial premixing, the equivalence ratio, and the hydrogen content on the burning velocity profiles and its characteristics of the partially premixed combustion process were investigated. The main conclusions are as follows:

1. As the *MFT* decreases, the degree of partial premixing of the mixtures increases, accelerating the heat release process. The partially premixed combustion process of the mixture effectively shortens the duration of various combustion stages. With the increase in the degree of partial premixing, the influence of the inhomogeneous concentration field and disturbed flow field on the combustion process becomes more dominant, leading to a significant increase in flame propagation speed. As the equivalence ratio and hydrogen content increase, the promoting effect of partial premixing weakens. The study also reveals that the effect of hydrogen content on the combustion duration of the mixture with different partial premixing degrees is different, which is closely related to hydrogen's high diffusivity and chemical reactivity.
2. The constant-pressure method is used to calculate the burning velocity of partially premixed mixtures in the complex confined combustion environments. The partially premixed burning velocities show a distinct single-peak characteristic, while the relatively stable propagation phase gradually shortens or even disappears, indicating that the combustion reactions are more concentrated in the early stages. With the increase

in the degree of partial premixing, the peak of the burning velocity $S_{T\text{-}max}$ increases and the peak moment $T - S_{T\text{-}max}$ is advanced. The degree of partial premixing of the mixture has the greatest influence on the initial combustion phase, and the promotion effect gradually diminishes as the combustion progresses.

3. As the *MFT* shortens, the degree of partial premixing increases, leading to a gradual increase in the $S_{T\text{-}max}$ and $R - S_{T\text{-}max}$. This also causes the $T - S_{T\text{-}max}$ to shift earlier, while the $T - S_{T\text{-}max}/T_{peak}$ continues to decrease. For mixtures with high equivalence ratios and high hydrogen content, the influence of partial premixing on the $R - S_{T\text{-}max}$ and $T - S_{T\text{-}max}/T_{peak}$ is the weakest. This indicates that under these conditions, the combustion process is primarily controlled by chemical reaction kinetics, and the influence of partial premixing is diminished. For mixtures with the same equivalence ratio and partial premixing degree, an increase in hydrogen content leads to a gradual reduction in the $R - S_{T\text{-}max}$. Moreover, as the degree of partial premixing increases, the influence of hydrogen content becomes more pronounced. This is because hydrogen's preferential diffusion effect significantly enhances flame propagation speed, particularly at low mixture equivalence ratios.
4. The peak of the burning velocity occurs almost simultaneously with the peak of the second-order derivative of the combustion pressure in the partially premixed combustion (R^2 = 0.992). This phenomenon indicates that the rapid increase in the combustion reaction rate directly drives the dynamic changes in combustion pressure. This correlation is basically independent of the mixture composition and the partial premixing process. However, the two peaks ($S_{T\text{-}max}$ and $(d^2p/dt^2)_{\max}$) show a nonlinear relationship. This nonlinearity may originate from the complex interactions between local concentration distributions and turbulent fields, as well as the heat release kinetics characteristics at different combustion stages.

Author Contributions: Investigation, data curation, writing—original draft preparation, writing—review and editing, conceptualization, visualization, validation, Y.L. (Yanfei Li), L.C. and Y.L. (Ying Liu); supervision, resources, project administration, X.Z.; software, methodology, L.C. All authors have read and agreed to the published version of the manuscript.

Funding: This work was supported by the National Natural Science Foundation of China (no. 51976008).

Data Availability Statement: Data will be available from the corresponding author upon reasonable request. All other data supporting this study are available within the article.

Acknowledgments: Particular acknowledgement goes to the organizers of the SDEWES 24 Conference for selecting the present paper for the *Energies* Special Issue publication.

Conflicts of Interest: The authors declare no conflicts of interest.

Nomenclature

A_b	Area of flame front (m^2)
c_{pu}	Constant-pressure specific heat capacity of unburnt mixture (J/(kg·K))
c_{vu}	Constant-volume specific heat capacity of unburnt mixture (J/(kg·K))
m_u	Mass of unburnt mixture (kg)
m_i	Mass of initial mixture (kg)
m_b	Mass of burnt mixture (kg)
p	Combustion pressure (MPa)
p_{max}	Peak combustion pressure (MPa)

V	Volume of the constant-volume combustion chamber (m^3)
V_u	Volume of unburnt mixture (m^3)
V_b	Volume of burnt mixture (m^3)
X_{H2}	Hydrogen content
R_b	Burnt flame radius (m)
R_u	Gas constant of unburned mixture (J/(kg·K))
R_v	Equivalent radius of a constant-volume combustion chamber (m)
$R - S_{T\text{-}max}$	The ratio of the $S_{T\text{-}max}$ under partially premixed conditions to that under premixed conditions for the same mixture composition
S_T	Burning velocity (m/s)
$S_{T\text{-}max}$	Maximum turbulent burning velocity (m/s)
S_T^i	Initial turbulent burning velocity (m/s)
$T - S_{T\text{-}max}$	Moment of maximum turbulent burning velocity (s)
$T_{initial}$	Initial combustion duration (s)
T_{main}	Main combustion duration (s)
$T_{gravity}$	Combustion center of gravity (s)
T_{peak}	Global combustion duration (s)
T_b	Burnt mixture temperature (K)
T_u	Unburnt mixture temperature (K)
T_i	Initial mixture temperature (K)

Greek Symbols

α	Thermal coefficient
β	Pressure coefficient
γ_u	Specific heat ratio of unburnt mixture
γ_b	Specific heat ratio of burnt mixture
ρ_u	Density of unburnt mixture (kg/m^3)
ρ_i	Density of initial mixture (kg/m^3)

Abbreviations

CVCC	Constant-volume combustion chamber
ICEs	Internal combustion engines
MFT	Mixture formation time
NCHR	Normalized cumulative heat release rate
RHRR	Representative heat release rate (MPa/s)
RTHR	Representative total heat release (MPa/s)

References

1. Ria, A.; Dini, P. A Compact Overview on Li-Ion Batteries Characteristics and Battery Management Systems Integration for Automotive Applications. *Energies* **2024**, *17*, 5992. [CrossRef]
2. Singla, M.K.; Nijhawan, P.; Oberoi, A.S. Hydrogen fuel and fuel cell technology for cleaner future: A review. *Environ. Sci. Pollut. Res.* **2021**, *28*, 15607–15626. [CrossRef] [PubMed]
3. Makaryan, I.A.; Sedov, I.V.; Salgansky, E.A.; Arutyunov, A.V.; Arutyunov, V.S. A Comprehensive Review on the Prospects of Using Hydrogen–Methane Blends: Challenges and Opportunities. *Energies* **2022**, *15*, 2265. [CrossRef]
4. Benajes, J.; Novella, R.; García, A.; Arthozoul, S. Partially Premixed Combustion in a Diesel Engine Induced by a Pilot Injection at the Low-pressure Top Dead Center. *Energy Fuels* **2009**, *23*, 2891–2902. [CrossRef]
5. Yin, L.; Lundgren, M.; Wang, Z.; Stamatoglou, P.; Richter, M.; Andersson, Ö.; Tunestål, P. High efficient internal combustion engine using partially premixed combustion with multiple injections. *Appl. Energy* **2019**, *233*, 516–523. [CrossRef]
6. Jin, S.; Li, J.; Deng, L.; Wu, B. Effect of the HPDI and PPCI Combustion Modes of Direct-Injection Natural Gas Engine on Combustion and Emissions. *Energies* **2021**, *14*, 1957. [CrossRef]
7. Seffrin, F.; Fuest, F.; Geyer, D.; Dreizler, A. Flow field studies of a new series of turbulent premixed stratified flames. *Combust. Flame* **2010**, *157*, 384–396. [CrossRef]
8. Sweeney, M.S.; Hochgreb, S.; Dunn, M.J.; Barlow, R.S. The structure of turbulent stratified and premixed methane/air flames II: Swirling flows. *Combust. Flame* **2012**, *159*, 2912–2929. [CrossRef]

9. Sweeney, M.S.; Hochgreb, S.; Dunn, M.J.; Barlow, R.S. The structure of turbulent stratified and premixed methane/air flames I: Non-swirling flows. *Combust. Flame* **2012**, *159*, 2896–2911. [CrossRef]
10. Meares, S.; Masri, A.R. A modified piloted burner for stabilizing turbulent flames of inhomogeneous mixtures. *Combust. Flame* **2014**, *161*, 484–495. [CrossRef]
11. Lipatnikov, A.N. Stratified turbulent flames: Recent advances in understanding the influence of mixture inhomogeneities on premixed combustion and modeling challenges. *Prog. Energy Combust. Sci.* **2017**, *62*, 87–132. [CrossRef]
12. Hu, Z.; Li, M.; Miao, X.; Wang, Z.; Tang, Y.; Wu, X.; Yu, W.; Kang, Z.; Deng, J. Influence of Ambient Pressure on the Jet-Ignition Combustion Performance and Flame Propagation Characteristics of Gasoline in a Constant Volume Combustion Chamber. *Energies* **2024**, *17*, 3101. [CrossRef]
13. Pasquier, N.; Lecordier, B.; Trinité, M.; Cessou, A. An experimental investigation of flame propagation through a turbulent stratified mixture. *Proc. Combust. Inst.* **2007**, *31*, 1567–1574. [CrossRef]
14. Balusamy, S.; Cessou, A.; Lecordier, B. Laminar propagation of lean premixed flames ignited in stratified mixture. *Combust. Flame* **2014**, *161*, 427–437. [CrossRef]
15. Balusamy, S.; Cessou, A.; Lecordier, B. Direct measurement of local instantaneous laminar burning velocity by a new PIV algorithm. *Exp. Fluids* **2011**, *50*, 1109–1121. [CrossRef]
16. Wang, J.; Huang, Z.; Zheng, J.; Miao, H. Effect of partially premixed and hydrogen addition on natural gas direct-injection lean combustion. *Int. J. Hydrogen Energy* **2009**, *34*, 9239–9247. [CrossRef]
17. Askari, O.; Metghalchi, H.; Hannani, S.K.; Moghaddas, A.; Ebrahimi, R.; Hemmati, H. Fundamental Study of Spray and Partially Premixed Combustion of Methane/Air Mixture. *J. Energy Resour. Technol.-Trans. ASME* **2013**, *135*, 9. [CrossRef]
18. Askari, O.; Metghalchi, H.; Hannani, S.K.; Hemmati, H.; Ebrahimi, R. Lean Partially Premixed Combustion Investigation of Methane Direct-Injection Under Different Characteristic Parameters. *J. Energy Resour. Technol.-Trans. ASME* **2014**, *136*, 7. [CrossRef]
19. Lee, S.; Kim, G.; Bae, C. Lean combustion of stratified hydrogen in a constant volume chamber. *Fuel* **2021**, *301*, 121045. [CrossRef]
20. Ge, R.; Hu, E.; Yao, X.; Tang, C.; Huang, Z. Ethanol stratified ultra-lean combustion with hydrogen enrichment in a constant volume vessel. *Fuel* **2024**, *357*, 129638. [CrossRef]
21. Bradley, D.; Hicks, R.A.; Lawes, M.; Sheppard, C.G.W.; Woolley, R. The Measurement of Laminar Burning Velocities and Markstein Numbers for Iso-octane–Air and Iso-octane–n-Heptane–Air Mixtures at Elevated Temperatures and Pressures in an Explosion Bomb. *Combust. Flame* **1998**, *115*, 126–144. [CrossRef]
22. Bradley, D.; Gaskell, P.H.; Gu, X.J. Burning velocities, Markstein lengths, and flame quenching for spherical methane-air flames: A computational study. *Combust. Flame* **1996**, *104*, 176–198. [CrossRef]
23. Iijima, T.; Takeno, T. Effects of temperature and pressure on burning velocity. *Combust. Flame* **1986**, *65*, 35–43. [CrossRef]
24. Bao, X.; Jiang, Y.; Xu, H.; Wang, C.; Lattimore, T.; Tang, L. Laminar flame characteristics of cyclopentanone at elevated temperatures. *Appl. Energy* **2017**, *195*, 671–680. [CrossRef]
25. Yin, L.; Turesson, G.; Tunestål, P.; Johansson, R. Evaluation and transient control of an advanced multi-cylinder engine based on partially premixed combustion. *Appl. Energy* **2019**, *233*, 1015–1026. [CrossRef]
26. Lewis, B.; von Elbe, G. Determination of the Speed of Flames and the Temperature Distribution in a Spherical Bomb from Time-Pressure Explosion Records. *J. Chem. Phys.* **1934**, *2*, 283–290. [CrossRef]
27. Saeed, K.; Stone, C.R. Measurements of the laminar burning velocity for mixtures of methanol and air from a constant-volume vessel using a multizone model. *Combust. Flame* **2004**, *139*, 152–166. [CrossRef]
28. Omari, A.; Tartakovsky, L. Measurement of the laminar burning velocityusing the confined and unconfined spherical flame methods—A comparative analysis. *Combust. Flame* **2016**, *168*, 127–137. [CrossRef]
29. Hinton, N.; Stone, R.; Cracknell, R. Laminar burning velocity measurements in constant volume vessels—Reconciliation of flame front imaging and pressure rise methods. *Fuel* **2018**, *211*, 446–457. [CrossRef]
30. Faghih, M.; Chen, Z. The constant-volume propagating spherical flame method for laminar flame speed measurement. *Sci. Bull.* **2016**, *61*, 1296–1310. [CrossRef]
31. Reyes, M.; Tinaut, F.V.; Horrillo, A.; Lafuente, A. Experimental characterization of burning velocities of premixed methane-air and hydrogen-air mixtures in a constant volume combustion bomb at moderate pressure and temperature. *Appl. Therm. Eng.* **2018**, *130*, 684–697. [CrossRef]
32. Sun, Z.-Y. Experimental studies on the explosion indices in turbulent stoichiometric H_2/CH_4/air mixtures. *Int. J. Hydrogen Energy* **2019**, *44*, 469–476. [CrossRef]
33. Huang, K.; Sun, Z.Y.; Tian, Y.-C.; Wang, K.-L. Turbulent combustion evolution of stoichiometric H_2/CH_4/air mixtures within a spherical space. *Int. J. Hydrogen Energy* **2020**, *45*, 10613–10622. [CrossRef]
34. Sun, Z.Y.; Xu, C. Turbulent burning velocity of stoichiometric syngas flames with different hydrogen volumetric fractions upon constant-volume method with multi-zone model. *Int. J. Hydrogen Energy* **2020**, *45*, 4969–4978. [CrossRef]
35. Wang, Y.; Li, W.; Chang, Q.; Cheng, J. Measurements of explosion parameters for diethyl ether/air mixtures at pre-ignition quasi-isotropic turbulence. *Fuel* **2021**, *292*, 120224. [CrossRef]

36. Xu, C.; Wang, H.; Zhou, K.; Li, X.; Zhou, W.; Liu, W.; Wang, C. Laminar Burning Velocity of Premixed Ethanol–Air Mixtures with Laser-Induced Spark Ignition Using the Constant-Volume Method. *Energy Fuels* **2019**, *33*, 7749–7758. [CrossRef]
37. Porowski, R.; Kowalik, R.; Nagy, S.; Gorzelnik, T.; Szurlej, A.; Grzmiączka, M.; Zielińska, K.; Dahoe, A. Deflagration Dynamics of Methane–Air Mixtures in Closed Vessels at Elevated Temperatures. *Energies* **2024**, *17*, 2855. [CrossRef]
38. Reyes, M.; Tinaut, F.V.; Melgar, A.; Pérez, A. Characterization of the combustion process and cycle-to-cycle variations in a spark ignition engine fuelled with natural gas/hydrogen mixtures. *Int. J. Hydrogen Energy* **2016**, *41*, 2064–2074. [CrossRef]
39. Zhang, B.; Wang, S.; Zhai, Y. Estimating the charge burning velocity within a hydrogen-enriched gasoline engine. *Int. J. Hydrogen Energy* **2023**, *48*, 10264–10271. [CrossRef]
40. Liang, C.; Li, X.; Xu, C.; Oppong, F.; Bao, Y.; Chen, Y.; Li, Y.; Wang, B.; Ge, J. Investigation of the Effects of Hydrogen Addition on Explosion Characteristics and Pressure Fluctuations of Ethyl Acetate. *Energies* **2024**, *17*, 5970. [CrossRef]
41. Huang, Z.; Wang, J.; Liu, B.; Zeng, K.; Yu, J.; Jiang, D. Combustion characteristics of a direct-injection engine fueled with natural gas–hydrogen blends under different ignition timings. *Fuel* **2007**, *86*, 381–387. [CrossRef]
42. Wang, Y.; Zhang, X.; Li, Y.; Qin, S. Experimental study on premixed turbulent flame of methane/air in a spherical closed chamber. *Energy Convers. Manag.* **2020**, *222*, 113219. [CrossRef]
43. O'Donovan, K.H.; Rallis, C.J. A modified analysis for the determination of the burning velocity of a gas mixture in a spherical constant volume combustion vessel. *Combust. Flame* **1959**, *3*, 201–214. [CrossRef]
44. Lewis, B.; Von Elbe, G. *Combustion, Flames and Explosions of Gases*, 3rd ed.; Academic Press, Inc.: Orlando, FL, USA, 1987.
45. Luijten, C.C.M.; Doosje, E.; de Goey, L.P.H. Accurate analytical models for fractional pressure rise in constant volume combustion. *Int. J. Therm. Sci.* **2009**, *48*, 1213–1222. [CrossRef]
46. Luijten, C.C.M.; Doosje, E.; van Oijen, J.A.; de Goey, L.P.H. Impact of dissociation and end pressure on determination of laminar burning velocities in constant volume combustion. *Int. J. Therm. Sci.* **2009**, *48*, 1206–1212. [CrossRef]
47. Wang, J.H.; Huang, Z.H.; Miao, H.Y.; Wang, X.B.; Jiang, D.M. Characteristics of direct injection combustion fuelled by natural gas-hydrogen mixtures using a constant no volume vessel. *Int. J. Hydrogen Energy* **2008**, *33*, 1947–1956. [CrossRef]
48. Huang, Z.; Shiga, S.; Ueda, T.; Nakamura, H.; Ishima, T.; Obokata, T.; Tsue, M.; Kono, M. Effect of Fuel Injection Timing Relative to Ignition Timing on the Natural-Gas Direct-Injection Combustion. *J. Eng. Gas Turbines Power* **2003**, *125*, 783–790. [CrossRef]
49. Fang, L.; Singh, H.; Ohashi, T.; Sanno, M.; Lin, G.; Yilmaz, E.; Ichiyanagi, M.; Suzuki, T. Effect of Machine Learning Algorithms on Prediction of In-Cylinder Combustion Pressure of Ammonia–Oxygen in a Constant-Volume Combustion Chamber. *Energies* **2024**, *17*, 746. [CrossRef]
50. Hwang, J.; Bae, C.; Park, J.; Choe, W.; Cha, J.; Woo, S. Microwave-assisted plasma ignition in a constant volume combustion chamber. *Combust. Flame* **2016**, *167*, 86–96. [CrossRef]
51. Li, Y.; Zhang, X.; Wang, Y. Experimental study on the combustion characteristics of premixed methane-hydrogen-air mixtures in a spherical closed chamber. *Fuel* **2021**, *299*, 120885. [CrossRef]
52. Zhang, J.; Abraham, J. A numerical study of laminar flames propagating in stratified mixtures. *Combust. Flame* **2016**, *163*, 461–471. [CrossRef]
53. Nagy, J.; Conn, J.W.; Verakis, H.C. *Explosion Development in a Spherical Vessel*; US Department of the Interior, Bureau of Mines: Washington, DC, USA, 1969; Volume 7279.

Disclaimer/Publisher's Note: The statements, opinions and data contained in all publications are solely those of the individual author(s) and contributor(s) and not of MDPI and/or the editor(s). MDPI and/or the editor(s) disclaim responsibility for any injury to people or property resulting from any ideas, methods, instructions or products referred to in the content.